Estd. 1962
"A++" Accredited by NAAC (2021)
with CGPA 3.52

SHIVAJI UNIVERSITY, KOLHAPUR

JOURNAL OF SHIVAJI UNIVERSITY : SCIENCE AND TECHNOLOGY

(Peer Reviewed Journal)

Volume-46, Issue-1 (January, 2020)

ISSN Science -0250-5347

JOURNAL OF SHIVAJI UNIVERSITY : SCIENCE AND TECHNOLOGY

(Peer Reviewed Journal)

Volume -46, Issue-1 (January, 2020)

ISSN Science -0250-5347

EDITORIAL BOARD OF THE JOURNAL

MEMBERS OF THE EDITORIAL BOARD

Estd. 1962
"A++" Accredited by NAAC (2021)
with CGPA 3.52

Shivaji University

Kolhapur 416 004 (INDIA)

JOURNAL OF SHIVAJI UNIVERSITY : SCIENCE AND TECHNOLOGY

(Peer Reviewed Journal)

Volume-46, Issue-1 (January, 2020)

ISSN Science -0250-5347

- Contact Details -
Prof. (Dr.) S. D. Delekar
Editor, Journal of Shivaji University : Science and Technology
and
Department of Chemistry
Shivaji University, Kolhapur 416 004 (India)
E-mail : editor.jscitech@unishivaji.ac.in
website : http://www.unishivaji.ac.in/journals/

Shivaji University, Kolhapur

JOURNAL OF SHIVAJI UNIVERSITY : SCIENCE AND TECHNOLOGY

(Peer Reviewed Journal)

Volume-46, Issue-1 (January, 2020)

ISSN Science -0250-5347

- Editor -
Prof. (Dr.) S. D. Delekar
Journal of Shivaji University :
Science and Technology

- Published by -
Dr. V. N. Shinde
Ag. Registrar,
Shivaji University, Kolhapur 416004.

- Printed by -
Shri. B. P. Patil
Superintend
Shivaji University, Kolhapur 416004.

The Editor, on behalf of the Editorial Board of the Journal of Shivaji University : Science and Technology, Vol. No. 46 (1) whises to express his thanks to the contributing authors and the experts for acting as referees for the papers included in the issue.

Published : July, 2023

Journal of Shivaji University : Science and Technology
Volume-46, Issue-1 (January, 2020)

INDEX

Department of Biochemistry

Shivaji University, Kolhapur

Journal of Shivaji University : Science & Technology

Volume-46, Issue-1 (January, 2020)

Departmental Editorial Board

Sr. No.	Name of the Faculty	Editorial Board Designation
1.	Prof. (Dr.) K. D. Sonawane	Chairman
2.	Prof. (Dr.) Mrs. J. P. Jadhav	Member
3.	Dr. (Mrs.) P. B. Dandge	Member
4.	Dr. P. K. Pawar	Member
5.	Dr. P. M. Gurao	Member
6.	Mr. S. S. Kale	Member

Extraction of Antifolate Antibacterial Compound, Benzylidene p-methoxyaniline from *Curcuma longa* L Leaves and Molecular Docking Study with Dihydrofolate Reductase

Assifa Shaikh[a], Naiem H. Nadaf[a], Nitin M. Naik[a], Maruti J. Dhanavade[a], Kailas D. Sonawane[b], Pradeep M. Gurao[b], Shailesh R. Waghmare[a,*]

[a]Department of Microbiology, Shivaji University, Kolhapur 416 004 (MS) India.
[b]Department of Biochemistry, Shivaji University, Kolhapur 416 004 (MS) India.
*Corresponding author**:** shlshwaghmare@gmail.com

ABSTRACT

Plants are rich source of secondary metabolites, with this intention we focused on the leaves of Curcumin longa L for the extraction of novel antimicrobial compound. Compounds showing antimicrobial activity were extracted in various solvents, but ethanol extract showed more potency. The compound extracted in ethanol was separated on TLC and identified as Benzylidene p-methoxyaniline using GC/MS. This compound has shown broad spectrum activity against P. aeruginosa, S. aureus, B. subtilis, S. typhimurium and P. vulgaris. The important aspect is that inhibitory activity was observed only at growing phase and not at stationary at very low concentration. In the mechanism of action study cell wall and DNA of the tested organism was not found to damage, but in-silico analysis gives insights on inhibition of dihydrofolate reductase. Thus, Benzylidene p-methoxyanilineantifolate antibacterial compound extracted from C. longa L could be a potential molecule for the control of antibiotic resistance pathogens.

KEYWORDS

Benzylidene p-methoxyaniline, C. longa, Antibacterial, MIC, Molecular docking.

…….

1. INTRODUCTION

Folic acid is essential for the synthesis of nitrogen base purines and pyrimidines and, consequently, for the synthesis of DNA [1]. The mammals possess an active transport system, utilizing membrane-associated folate transport proteins [2], in plants and most micro-organisms folate must be synthesized de novo through the folate biosynthetic pathway. The presence of this pathway in many pathogenic micro-organisms and, crucially, its absence in mammals, that has made the folate pathway attractive for antimicrobial drug target [3].

Turmeric (*Curcuma longa* L) is a rhizomatous herbaceous perennial plant of the ginger family Zingiberaceae native in South India. It is distributed through tropical and subtropical regions of the world being widely cultivated in Asian countries mainly in India and China. In India it is popularly known as 'Haldi'. It is also cultivated in Malaysia, Indonesia and India due to its economic importance. Jayaprakash et al., (2005) described the chemistry and biological activity of leaf, stalk and rhizome of *Curcuma longa* L. Literature survey insights the use of *C. longa* in traditional medicines since long time [4-7]. Turmeric powder is known for antimicrobial, anti-inflammatory, antiseptic properties and being used since ancient times in the Indian system of medicine to treat variety of diseases [8].

Antibiotic resistance has emerged with faster rate, so there is considerable interest to investigate the antimicrobials from different extracts against a range of bacteria to develop safe and natural antimicrobial substances useful for infectious control [9]. Cowan in 1999 reviewed that the plants are rich source of antimicrobial compounds such as phenolics, quinones, flavonoids, tannins, coumarins, terpenoids, alkaloids, lectins and polypeptides [10]. Hence, present work deals with extraction, characterization of novel antimicrobial compound from the leaves of *C. longa* L and to study its antimicrobial properties against antibiotic resistant pathogens.

2. EXPERIMENTAL SECTION

2.1. Organic solvent extraction

The leaves of *C. longa* L were collected from Mouje Sangaon region Dist. Kolhapur, Maharashtra, India. Collected leaves were washed and kept into oven at 50 ºC. After complete removal of water, leaves were grinded and powder was kept in container for further use. This powder was used for the extraction of antimicrobial compounds in different organic solvents such as Acetone, Ethanol, Petroleum ether, Chloroform, Ethyl acetate, Methanol and Distilled water. The 0.5gm of powder was added into the 25ml organic solvent each and kept into freeze for 12 hrs. After 12 hrs the extracts were centrifuged at 8000 rpm for 15 min. and supernatant was collected. The collected supernatant was concentrated and tested for antibacterial activity.

2.2. Anti-bacterial study

The antibacterial activity of various organic solvent extracts such as chloroform, methanol, petroleum ether, ethyl acetate, ethanol and aqueous extract was carried out by agar cup method. The reference microorganisms such as *P. aeruginosa, S. aureus, B. subtilis, S. typhimurium, P. vulgaris* were used to test antibacterial activity in present study. Each solvent extracts volume of 25µl, 50µl, 100µlwere added at in the wells along with their respective solvent as control. Plates were kept for diffusion of sample in refrigerator for 15 min and then incubated at 37°C for 24 hrs. After incubation period plates were observed for zone of inhibition.

2.3. Separation of compounds by TLC

Ethanol extract was loaded on TLC and solvent system used was Chloroform: Acetic acid in 9:1 ratio. The chromatogram was developed by using iodine chamber and after development of plate, compounds were separated and mixed with 5 ml of ethanol and centrifuged at 5000 rpm for 15 min. Collected supernatant was allowed to concentrate and each separated compound has then tested for antimicrobial properties.

2.4. GC-MS analysis

The compound separated through TLC was identified by using QP-2010 gas chromatography coupled with mass spectroscopy (Shimadzu). The ionization voltage was 70ev. Gas chromatography was conducted by temperature programming made with Rtx-5Ms column (60m×250µmi.d.× 0.25µm film thickness). Carrier gas was He (1 ml^{-1}) and chromatographic conditions were as follows; initial oven temperature was maintained at 80 °C for 5 min and subsequently programmed from 80 °C to 150 °C at a rate of 3 °C min^{-1} and 10 °C min^{-1} from120 to 280 °C where it was held for another 10 min. Injector temperature: 250 °C; mass range: 40–650 amu; solvent delay: 4 min.; electron impact at 70ev. The compound was identified on retention time and fragmentation patterns available on NIST spectral library.

2.5. Determination of MIC

The minimum inhibitory concentration (MIC) of Benzylidene-p-methoxy aniline for different pathogenic organisms such as *P. aeruginosa, B. subtilis, S. typhimurium, S. aureus* and *P. vulgaris* was checked at different concentrations like0.2, 0.4, 0.6, 0.8 and 1 µg/ml. The 5 ml sterile nutrient broth adjusted with respective concentrations and 0.1 ml suspension of test organisms were added (10^6 cells). Control sets of all tests organisms were maintained without addition of compound and then all tubes were incubated at 37 ºC for 24 hrs. After incubation the optical density was measured at 530nm and minimum concentration inhibiting the growth of organism noted as MIC.

2.6. Mechanism of inhibition

2.6.1. Cell lysis study

The purified compound was used to study its mechanism of action on the pathogenic organisms. The *S. aureus* was used as model organism inoculated in nutrient broth and incubated at 37 ºC for 24 hrs. After incubation period the cells were separated by centrifugation at 8000 rpm for 15 min. and washed with saline water. Then the collected cells were suspended in 50 ml saline water containing Benzylidene-p-methoxyaniline at 20 µg/ml concentration and flask was incubated at 37 ºC. After 1hr incubation 2ml aliquot was taken and centrifuged at 8000rpm for 15 min. The

obtained supernatant was subjected to the determination of protein content by Bradford assay [11]. The aliquots were collected continuously for 12 hrs to determine protein content. The same flask run without addition of Benzylidene-p-methoxyaniline was kept as control.

2.6.2. In-vitro DNA damage study

To study the DNA damage ability of Benzylidene-p-methoxyaniline, DNA was isolated from *S. aureus* as per method described by Shahriar et al. (2011) [12]. In test,10µl of freshly isolated DNA was added with 5µl (40µg/ml) purified Benzylidene-p-methoxyaniline and incubated at 37 ºC for 60 min. The positive control runs with hydrogen peroxide (H_2O_2) and negative control as DNA. The DNA damaged have been analysed by agarose gel electrophoresis (0.8%) and bands were visualized by ethidium bromide.

2.6.3. Molecular docking studies

The use of computational approaches to understand molecular interactions between enzyme and ligand have been found useful in many studies [13-20]. In this respect we have done molecular docking studies to find out interactions between dihydrofolate reductase (2w9t.pdb) [21] and Benzylidene p-methoxyaniline using Autodock [22]. The SPARTAN ver 6.0.1 Software [23] was used to build the three-dimensional model of Benzylidene p-methoxyaniline and minimized by Hartree Fock (HF) method using SPARTAN [24]. Then finally the minimized structure of Benzylidene p-methoxyaniline was used in a docking experiment with dihydrofolate reductase (2w9t.pdb) [15]. Then structural analysis of docked complex of dihydrofolate reductase (2w9t.pdb) with Benzylidene p-methoxyaniline was carried out using CHIMERA [25]. The CHIMERA software was used to study the interactions of dihydrofolate reductase active site residues with Benzylidene p-methoxy aniline.

2.6.4. Statistical analysis

Results obtained were the mean of three determinants and ANOVA was carried on all data at $p<0.05$ using GraphPad Software.

3. RESULTS and DISCUSSION

3.1. Antibacterial activity of crude extract

Turmeric has been known traditionally as a source of pharmaceutically active ingredient. Extracts prepared in various solvents such as methanol, chloroform, acetone, ethyl acetate, petroleum ether, ethanol and distilled water were differ in its antibacterial activity against different microorganisms as shown in **Table-1**. Among all extracts, ethanol extract showed promising antimicrobial activity against all tested

microorganisms and it was chosen for further study. The maximum antimicrobial activity was observed against *P. vulgaris* and *S. aureus* at 100µl volume. Methanol extract showed activity towards Gram negative pathogens such as *P. aeruginosa*, *S. typhimurium* and *P. vulgaris*, whereas Ethyl Acetate extract showed activity only against Gram positive pathogens like *B. subtilis* and *S. aureus*. Chloroform extract showed activity against *B. subtilis*. The aqueous extract moderately active against *P. aeruginosa*, *S. typhimurium*, *B. subtilis* and *S. aureus* similar to that of acetone extract. Earlier reports on crude leaf extract of *C. longa* suggested the presence of rich secondary metabolites such as alkaloids, terpenoids, phenolics and flavonoids [26-29].

Test organisms	Zone of inhibition in mm							
	Extract Vol (µl)	Acetone	Ethanol	Petroleum ether	Chloroform	Ethyl acetate	Methanol	D/W
P. aeruginosa	25	-	-	-	-	-	-	-
	50	-	7	-	-	-	-	-
	100	8	10	-	-	-	9	8
B. subtilis	25	-	-	-	-	-	-	-
	50	-	-	-	7	-	-	-
	100	7	9	7	10	9	-	9
S. typhimurium	25	-	6	-	-	-	-	-
	50	-	8	-	-	-	-	7
	100	10	10	7	-	-	8	10
S. aureus	25	-	8		-	-	-	-
	50	-	10		-	-	-	-
	100	8	12	9	-	8	-	6
P. vulgaris	25	-	-	-	-	-	-	-
	50	-	8	-	-	--	-	-
	100	-	11	-	-		10	-

Table-1. Antimicrobial activity of various organic solvent extract.

3.2. Purification of antimicrobial compound

The compounds were separated from ethanol extract by using thin layer chromatography. **Figure-1** showed the separation of various compounds on TLC. These compounds were further tested for antimicrobial activity. The separated compound showed broad spectrum antimicrobial activity against the *P. aeruginosa*, *S. aureus*, *B. subtilis*, *S. typhimurium* and *P. vulgaris* (**Table-2**).

It indicates that the purified compound is more active against *S. aureus* as compared to other pathogens. This data revealed that the efficiency of compound has been increased after separation through thin layer chromatography. The identification of purified antimicrobial compound was carried out by GC-MS analysis. The chromatogram showed presence of single peak at the retention time of 24.58 (**Figure-2a**). The NIST mass spectra library confirmed the molecule 356 mass peak (**Figure-2b**) with molecular weight 211 i.e. Benzylidene-p-methoxyaniline(**Figure-2c**). Before this, Awasthi and Dixit reported different types of biologically active molecules from the *C. longa* leaves oil [30] whereas Benzylidene-p-methoxyaniline reported first time in present study. Yunnikova et al., 2015 [31] has reported the Benzylidene-4-methoxyaniline as an intermediate product during the synthesis of 4-(7-cyclohepta-1,3,5-trienyl)-N-(1-cyclohepta-2,4,6-trienyl) aniline having antimicrobial activity. Recently, insect antifeedant activity of Benzylidene-p-methoxyaniline derivatives has been reported [32].

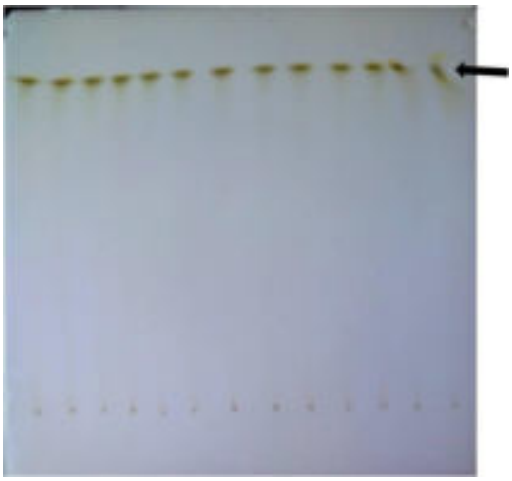

Figure-1. TLC analysis of ethanol extract. Compounds from ethanol extract were separated on TLC by using Chloroform: Acetic acid (9:1) solvent system and separated compounds were detected by using iodine chamber.

Table-2. Antimicrobial activity of crude and purified compound.

Test organisms	Zone of inhibition in mm	
	Crude	Purified
P. aeruginosa	09.66 ± 0.333	15.00 ± 0.577
S. aureus	11.33 ± 0.881	17.66 ± 0.666
B. subtilis	08.33 ± 0.333	13.66 ± 0.333
S. typhimurium	10.00 ± 0.577	16.00 ± 0.577

P. vulgaris	10.66 ± 0.666	15.00 ± 0.577

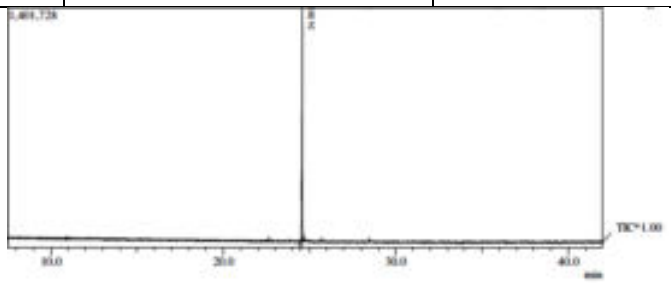

a

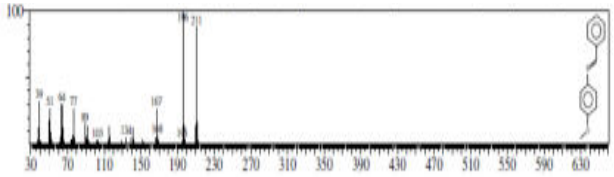

b

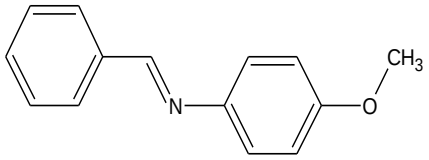

c

Figure-2. GCMS analysis of separated compound. a) Gas chromatogram of purified compound b) Mass spectra of Benzylidene-p-methoxyaniline c) structure of Benzylidene-p-methoxyaniline.

3.3. Determination of MIC

The purified compound was subjected to determination of MIC against different pathogenic organisms. For this purpose, the concentrations were used between 0.2–1.0µg/ml. **Figure-3** shows MIC for *S. aureus* and *S. typhimurium* 0.4µg/ml, *P. aeruginosa* and *P. vulgaris* 0.6µg/ml, whereas for *B. subtilis* was1.0 µg/ml. These results revealed that the compound is more effective against *S. aureus* and *S. typhimurium* at very low concentration, compared to other pathogens. It was found that the inhibitory concentration of molecule changes with susceptible pathogens. This suggests the broad-spectrum activity of compound, irrespective of inhibitory against specific group of bacteria. Earlier Bowkar et al., (2009) [33] reported three antifolate compounds having MIC in the range of 0.015- 0.25 against MRSA,

whereas Navarro-Martinez et al., (2005) [34] showed strong antibiotic activity against *Stenotrophomonas maltophilia*having MIC range 4 to 256µg/ml.

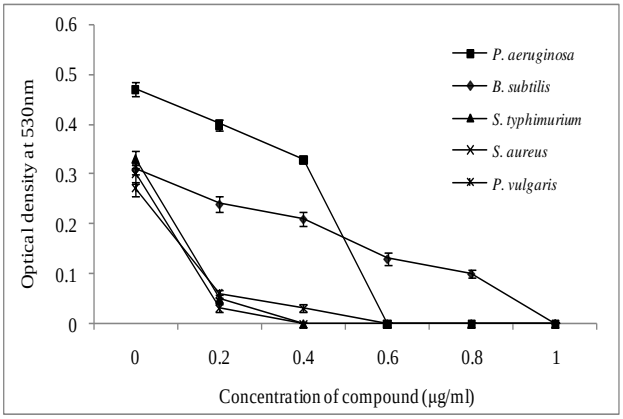

Figure-3. MIC of purified Benzylidene-p-methoxyaniline against pathogens. The different concentrations i.e., 0.2, 0.4, 0.6, 0.8 and 1 µg/ml of purified compound were added in the medium containing with pathogens and after incubation the optical density was measured at 530nm to determine MIC.

3.4. Mechanism of inhibition

The mechanism of action of compound was studied for its cell wall lysis action, by allowing molecule to interact with the surface of organism. After interaction, to detect cell wall lysis or cell membrane damage, the released cytoplasmic content was determined. The protein content was not found to increase after the interaction with compound, which indicates that the cell surface was not damaged by Benzylidene-p-methoxyaniline. In in-vitro DNA damage assay, from fig-4 it was seen that the DNA was found to be intact after interaction with compound, which reveals that Benzylidene-p-methoxyaniline does not damages the DNA to kill bacteria.

Antibacterial compound extracted from *C. longa* leaves showed structural similarity with Trimethoprim, so the compound was selected for antifolate mechanism by *In-silico* method. So Dihydrofolate reductase (DHFR) was focused for further analysis. Earlier Navarro-Martinez et al., (2005) [34] reported antifolate activity of epigallocatechin gallate from tea, which is efficient inhibitor of *S. maltophilia* DHFR. The MBC data revealed that the compound was efficiently inhibitory to organism at the time of exponential growth phase. So, this molecule could inhibit protein synthesis, DNA replication, mRNA synthesis or metabolic pathways at logarithmic phase.

Figure-4. In-vitro DNA damage analysis of pathogenic DNA. C- control DNA, P-H2O2 treated DNA, T- Benzylidene-p-methoxyaniline treated DNA. All these samples were run on Agarose gel electrophoresis (0.8%) and located DNA identified by using ethidium bromide under transilluminator.

3.5. Analysis of docked complexes of dihydrofolate reductase from *Staphylococcus aureus* with Benzylidene p-methoxyaniline

Molecular docking studies were carried out between dihydrofolate reductase (2w9t.pdb [21] and energy minimized Benzylidene p-methoxyaniline structure using Autodock [22]. The docked complex of dihydrofolate reductase and Benzylidene p-methoxyanilinewas stabilized by hydrogen bonding interactions. These hydrogen bonding interactions were further analyzed by using CHIMERA [25], which showed that active site residues of dihydrofolate reductase such as ASP 27, PHE 92 and THR 111 having strong hydrogen bonding interactions with the Benzylidene p-methoxyaniline (**Figure-5** and **Table-3**). Along with these, other residues of dihydrofolate reductase like ALA 7, ILE 14, PRO 21, HIS 23, LEU 24, TYR 98, ILE 113 and PHE 117 also interact with the Benzylidene p-methoxyaniline support the stability of docked complex (**Figure-5** and **Table-3**). Benzylidene p-methoxyaniline interacts with DHFR showing potent antifolate activity, which gives broad spectrum antibacterial nature against various tested pathogens.

Table-3. Hydrogen bonding interactions between dihydrofolate reeducates (2w9t.pdb).

Sr. No.	Interaction between active site residues of dihydrofolate reductase (2w9t.pdb) with Benzylidene p-methoxyaniline	Distance in Å
1	PRO 21.B CB ------ UNL 1.het H:	2.421
2	ASP 27.B OD1 ------ UNL 1.het H:	2.454
3	LEU 24.B CD2 ------ UNL 1.het C:	2.626
4	HIS 23.B HD1 ------ UNL 1.het C:	2.673
5	UNL 1.het C ------ ALA 7.B CB:	2.640
6	UNL 1.het C ------ TYR 98.B HH:	2.414
7	ILE 14.B CG2 ------ UNL 1.het C:	2.866
8	UNL 1.het O ------ PHE 117.B CZ:	2.687
9	UNL 1.het O ------ ILE 113.B CD1:	2.560
10	THR 111.B HG1 ------ UNL 1.het C:	2.449
11	PHE 92.B CE1 ------ UNL 1.het C:	2.543

Figure-5. Docked complex of dihydrofolate reductase (2w9t.pdb) (slate blue) with Benzylidene p-methoxyaniline (magenta).

4. CONCLUSION

The present study concludes that leaves of *C. longa* L is a rich source of antifolate antibacterial compound, Benzylidene-p-methoxyaniline. This compound has a broad-spectrum antibacterial activity and easily purified by simple techniques such as solvent extraction and TLC. In-Silico study reveals strong interaction of Benzylidene-p-methoxyaniline with dihydrofolate reductase, which confirms antifolate action. Thus, these results suggest that Benzylidene-p-methoxyaniline could be a promising molecule to develop novel therapeutic agent to control antibiotic resistant pathogens.

ACKNOWLEDGEMENT

All authors are very much thankful to Department of Science and Technology, New Delhi for financial support under the DST-PURSE scheme sanctioned to Department of Microbiology, Shivaji University, Kolhapur. KDS gratefully acknowledges University Grants Commission, New Delhi for financial support under the UGC-SAP-DRS-II scheme sanctioned to Department of Biochemistry, Shivaji University, Kolhapur, Maharashtra, India.

REFERENCES

1. Murray, P. R., Rosenthal, K. S., Pfaller, M. A. In Microbiologia Médica, edited by Mosby. Elsevier, (2006) pp.1756-1763.
2. Henderson, G. B., Huennekens, F. M. (1986) Methods in Enzymology, 122, 260–
   269.
3. Bermingham, A., Derrick, J. P. (2002) BioEssays, 24, 637–648.
4. Jayaprakasha, G. K., Rao, L. J. M., Sakariah, K. K. (2005) Trends in Food Science and Technology, 16, 533–548.
5. Eigner, D., Scholz, D. (1999) Journal of Ethanopharmacology, Phytochemistry and Pharmacology, 67, 1–6.
6. Ammon, H. P. T., Anazoda, M. I., Safayhi, H., Dhawan B. N., Srimal, R. C. (1992) Planta Medica, 58, 26–28.
7. Ammon, H. P. T., Wahl, M. A. (1991) Planta Medica, 57, 1–7.
8. Anon. In A Dictionary of Indian Raw Materials and Industrial Products, edited by Anon. The Indian Medical Gazette, (2001) pp.264–293.
9. Yap, P. S. X., Yiap, B. C., Ping, H. C., Lim, S. H. E. (2014) Open Microbiology
   Journal, 8, 6-14.
10. Cowan, M. M. (1999) Clinical Microbiology Reviews, 12, 564–582.
11. Bradford, M. M. (1976) Analytical Biochemistry, 72, 248-254.
12. Shahriar, M., Haque, R., Kabir, S., Dewan, I., Bhuyian, M. (2011) Journal of Pharmaceutical Sciences, 4, 53-57.
13. Sonawane, K. D., Dhanavade, M. J. In Computational approaches to understand
    cleavage mechanism of amyloid beta (Aβ) peptide, edited by Roy K. Springer, (2017) pp.263-282.
14. Parulekar, R. S., Barage, S. H., Jalkute, C. B., Dhanavade, M. J., Sonawane, K. D. (2013) The Protein Journal, 32, 467-476.
15. Barage, S. H., Sonawane, K. D. (2015) Neuropeptides, 52, 1-18.

16. Jalkute, C. B., Barage, S. H., Sonawane, K. D. (2015) Royal Society of Chemistry Advances, 5, 10488-10496.
17. Barage, S. H., Jalkute, C. B., Dhanavade, M. J., Sonawane, K. D. (2014) International Journal of Peptide Research and Therapeutics, 20, 409-420.
18. Dhanavade, M. J., Sonawane, K. D. (2014) Amino Acids, 46, 1853–1866.
19. Sonawane, K. D., Dhanavade, M. J. In Molecular docking technique to understand enzyme-ligand Interactions by Dastmalachi, S., Hamzeh-Mivehroud, M., Sokouti, B. Pharmaceutical Sciences, (2017) pp.245-264.
20. Dhanavade, M. J., Parulekar, R. S., Kamble, S. A., Sonawane, K. D. (2016) Molecular BioSystems, 12, 162-168.
21. Heaslet, H., Harris, M., Fahnoe, K., Sarver, R., Putz, H., Chang, J., Subramanyam, C., Barreiro, G., Miller, J. R. (2009) Proteins, 76, 706-717.
22. Morris, G. M., Huey, R., Lindstrom, W., Sanner, M. F., Belew, R. K., Goodsell, D. S., Olson, A. J. (2009) Journal of Computational Chemistry, 30, 2785-2791.
23. Hehre, J., Radom, W. L., Schleyer, P. V. R., Pople, J. A. (1976) Molecular Orbital Theory, 9, 399-406.
24. Slater, J. (1951) Physical Review Journals, 81, 385–390.
25. Pettersen, E. F., Goddard, T. D., Huang, C. C., Couch, G. S., Greenblatt, D. M., Meng, E. C., Ferrin, T. E. (2004) Journal of Computational Chemistry, 25, 1605-1612.
26. Oguntimein, B. O., Weyerstahl, P., Weyerstahl, H. M. (1990) Flavour and Fragrance Journal, 5, 89–90.
27. McCarron, M., Mills, A. J., Whittaker, D., Sunny, T. P., Verghese, J. (1995) Flavour and Fragrance Journal, 10, 355–357.
28. Garg, S. N., Mengi, N., Patra, N. K., Charles, R., Kumar, S. (2002) Flavour and Fragrance Journal, 17, 103–104.
29. Mazumder, R., Mendiratta, T., Mondal, S. C., Mazumder, A. (2000) Ancient Science of Life, 20, 92-96.
30. Awasthi, P. K., Dixit, S. C. (2009) Journal of Young Pharmacists, 1, 312-316.
31. Yunnikova, L. P., Akenteva, T. A., Ésenbaeva, V. V. (2015) Pharmaceutical Chemistry Journal, 49, 243-245
32. Lakshmanan, K., Sekar, K. G., Sathiyendiran, V., Suresh, R. (2015) International Letters of Chemistry, Physics and Astronomy, 41, 118-123.
33. Bowker, K. E., Caspers, P., Gaucher, B., MacGowan, A. P. (2009) Antimicrobial Agents and Chemotherapy, 53, 4949–4952.
34. Navarro-Martinez, M. D., Navarro-Peran, E., Cabezas-Herrera, J., Ruiz-Gomez, J., Garcia-Canovas, F., Rodriguez-Lopez, J. N. (2005) Antimicrobial Agents and Chemotherapy, 49, 2914–2920.

Isolation, characterization, and partial purification of xylanase from *Cellulomonas flavigena* NCIM 2481

Geetanjali T. Mali[a], Pramod J. Kasabe[a], Apurva D. Patil[a], Padma B. Dandge[a,*]

[a]Department of Biochemistry, Shivaji University, Kolhapur 416 004 (MS) India.

*Corresponding author: pbd_biochem@unishivaji.ac.in

ABSTRACT

The xylans are the most widespread hemicelluloses and are considered to be the second most plentiful biopolymers in the plant kingdom. Xylan is hetero-polysaccharide containing a backbone structure of ß-1, 4-linked D-xylose residues and short side chains of sugars are cooperatively referred to as the ß-1, 4-D-xylans. Xylans have been suggested to play avital role in the aggregation pattern of cellulose, which affects the crystalline structure and changes the magnitude of cellulose fibrils. The Endo-1, 4-ß-xylanase is the most important xylan degrading enzyme, that cleave the internal glycosidic linkages of the heteroxylan backbone. Now a days xylanase is one of the most imperative enzyme in paper industries to increase the brightness of paper and invaluable need in food processing industries mainly for extraction and clarification of fruit juices and wines. The present study evaluates the potentxylanase producing strain from Cellulomonas sp. Among them Cellulomonas flavigena NCIM 2481 shows maximum enzyme activity (40.6 U) at 7th day of incubation with specific activity 25.81 U/mg. While partial purified xylanase showed specific activity of 34.87 fold. Optimized conditions of xylanase like pH, temp and Km were studied for characterization of enzyme and are found to be 6.8, 50°C and 2.78 mg/ml. respectively.

KEYWORDS

Cellulomonas flavigena, Xylan, Xylanase, Km, DEAE cellulose.

…….

1. INTRODUCTION

The plant cell wall is at a standstill of three major polymeric components, cellulose (35-50%), hemicelluloses (20-30%) and lignin (20-30%) [1]. Hemicelluloses are plenteous polysaccharides in nature next to cellulose. They occur in close association with cellulose and lignin and furnish to the rigidity of plant cell walls in lignified tissues. Hemicelluloses are composed of noncellulosic polysaccharides these are glucans, mannans and xylans [2], among these xylan is the major constituent of hemicelluloses. Up to 35% of the dry weight of higher plants is made up of xylan,

which is composed of short side chains of O-acetyl, -L-arabinofuranosyl, and D-glucuronyl or O-methyl-D-glucuronyl residues and a homopolymeric backbone chain of 1,4-linked -D-xylopyranose units [3].

The cooperative action of multiple enzymes is required for the complete hydrolysis of xylan, enlistendo-β-1,4-xylanase (EC 3.2.1.8), β-xylosidase (EC 3.2.1.37) and a series of enzymes that degrade side chain groups. Among these, endo-β-1,4-xylanase is the key enzyme that having specificity to cleaves internal glycosidic linkages to produce short chain xylooligo saccharides of various lengths [4] and because small molecular weightcaneasily pass through the pores of hemicellulose associated network and causes efficient hydrolysis of xylan [5].

Xylanase is significant enzyme due to theirbroad spectrumindustrial applications. The most important application of xylanase is in prebleaching of kraft pulp to moderate the treatment of chemicals and to increase the brightness of paper [6]. Along with paper and pulp industry xylanase is also used as food additives in wheat flour for improving quality of baked products by helping the redistribution of water and leaving the dough softer and easier to knead [7]. In animal feeds, xylanase increases the digestibility of feed with decrease in viscosity [8]. Xylanase have substantial applications inextraction of juices, coffee flavors, spices, oils and pigments as well as clarifications of juices and wines [9]. A mixture of xylanase and specialized enzymes are required in bioconversion processes that catalyze maximum hydrolysis of complex substrates to yield the monomeric residues for biofuel fermentation [10].

Xylanase enzymes, which are generated by numerous genera and species of bacteria, fungi, and actinomycetes, are abundant in microorganisms. High quantities of extracellular xylanase are secreted by a number of Bacillus species.

The present study is to uncover the capacity of *Cellulomonas* sp. for the production of the study enzyme.

2. EXPERIMENTAL SECTION

2.1 Chemicals and media components

Birchwood xylan, xylose, 3,5 Dinitrosalicylicacid was purchased from Sigma chemical co. DEAE Cellulose-52 and all other analytical grade chemicals purchased from Himedia Co. and Local suppliers in India.

2.2 Organism maintenance and Growth Conditions

The culture of*Cellulomonasflavigena*NCIM2481 used for xylanase production was obtained from National Collection of Industrial Microorganisms, NCL, Pune, (M.S.) India. The strain was cultured and maintained on nutrient agar (NA).

2.3 Cultivation of *Cellulomonas flavigena* NCIM 2481

The 250 ml Erlenmeyer flask containing 100 ml basal media (in g/lit: $NaNO_3$,0.753; KH_2PO_4, 3.3; $MgSO_4.7H_2O$, 0.423; $CaCl_2.2H_2O$,0.42) with 1% xylan was used for the production of enzyme. The culture was grown for 24 hrs in nutrient broth and used as an inoculum. 1% inoculum was added in the 100ml production medium and incubated at R.T. on rotary shaker at 120 rpm for 160 to180 hrs [11]. The enzyme was harvested by centrifugation at 8000 rpm for 15 mins and used as crude enzyme.

2.4 Enzymatic assay and Protein estimation:

The xylanase activity was assayed by using 1% birch wood xylan as substrate. The reaction mixture containing 1 ml substrate, 1.5ml phosphate buffer of pH 6.8 and 0.5 ml enzyme was incubated at 40°c for 30 min. the amount of reducing sugar liberated was estimated by 3,5Dinitro salicylic acid (DNSA) method [12]. Xylanase enzyme activity was defined as the µg of xylose released per ml of enzyme per min under specific assay conditions. Protein content of the enzymatic extract was estimated by using lowery method with bovine serum albumin as a standard [13].

2.5 Partial purification of xylanase:

The purification of enzyme was carried out at 4˚C, the fermented nutrient broth containing xylanase was subjected to centrifuge at 10,000rpm in cooling centrifuge at 4˚C for 10 min to obtain cell free medium. Supernatant was collected and pellet was discarded. And the supernatant is pooled for further purification steps.

2.5.1 Ammonium sulphate precipitation and dialysis

This procedure involved continuously stirring at 4 °C while adding 50, 60, 70, and 80 percent ammonium sulphate to 10 ml of each centrifuged broth until precipitation occurred. To get a precipitated pellet, the precipitated material was centrifuged at 8000 rpm for 10 min at 4 °C. The enzyme activity and protein concentration were assessed using the Lowery technique and DNSA, respectively, after the pellet had been dissolved in 5 ml of 0.1 M phosphate buffer (pH 6.6). On a magnetic stirrer for 6 to 8 hours at 4 degrees Celsius, the material was dialyzed against 0.1 M phosphate buffer. Every two hours, the buffer was modified. Then, as previously mentioned, the enzyme activity and protein concentration were calculated.

2.5.2 Ion Exchange Chromatography

For purification, a DEAE cellulose anion exchanger column was employed. 0.1 M phosphate buffer had been used to pre-equilibrate the column. Elution fractions of 5 ml each were collected at a flow rate of 1 ml/min after the dialyzed sample was placed onto the column and processed with 0.1M phosphate buffer at pH 6.6. Continual salt gradients of 0.1M, 0.2M, 0.3M, 0.4M, and 0.5M NaCl were used to elute the protein attached to the DEAE cellulose column. By measuring absorbance at 280 nm using a UV-visible spectrophotometer, the protein content of the samples

was found. The active fractions containing higher protein content were pooled for determination of enzyme activity by using DNSA method.

2.6 Optimization of enzyme

The enzyme was put through a variety of permutations and combinations of the assay conditions, including a pH range from acidic to alkaline and temperature changes from line to room temperature.

2.6.1 Effect of pH and temperature on enzyme activity

The optimum pH of purified xylanase was assayed with birch wood xylanas substrate at different pH ranging from 6.0 - 7.8 with incremental level of 0.2pH., following buffers were employed for optimization: 0.1M sodium acetate, pH 4.0-6.0;0.1M potassium phosphate, pH 6.0-7.0, and 0.1M Tris-HCl, pH 7.5-9. Enzyme assay was conceded by DNSA method using these different buffers and incubating the tubes at 40˚C for 30 minutes. The optimum temperature of enzyme was determined by incubating the reaction mixture in 0.1 M phosphate buffer at various temperatures ranging from20˚C - 80˚C for 30 minutes.

2.6.2 Determination of Km

The influence of birch wood xylan concentration ranging from 1 to 10 mg/ml on xylanase activity was resolved under the optimum assay conditions (50°C, pH 6.8 for 30 min). According to Lineweaver-burk plot Km of enzyme was predicted by linear regression from double reciprocal plot [14].

3. RESULT AND DISCUSSION

3.1 Evaluation of potent xylanase producers among *Cellulomonas* sp and optimization of media

All the four strains of *Cellulomonas* sp. were quantitatively screened for maximum enzyme production containing 1% xylan under submerged fermentation conditions, in which *Cellulomonas flavigena* NCIM 2481 showed significant increase in enzyme activity (40.6 IU/ml).

3.2 Effect of time duration on enzyme activity

In order to determine the period required for maximum production of enzyme, basal media containing 1% xylan was used. The period required for is shown in **Figure-1**. The xylanase enzyme shows maximum enzyme activity (40.6 IU/ml) at 7^{th} day of incubation in basal media containing 1% xylan. The enzyme activity was declined after further incubation of broth. Similar results were reported for the production of xylanase and cellulose from *Cellulosimicrobium cellulans* grown in pretreated and extracted bagasse and minimal nutrient medium [15].

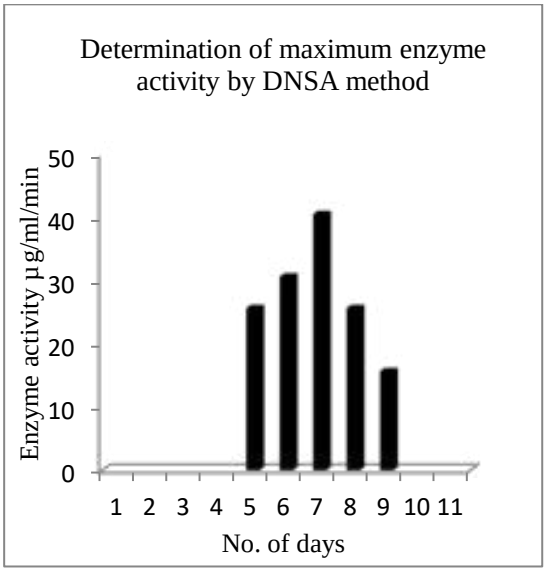

Figure-1. Effect of incubation time on enzyme activity.

3.3 Partial Purification of enzyme

3.3.1 Ammonium sulphate precipitation and dialysis

The crude enzyme was precipitated by addition of 50%, 60%, 70%, 80% ammonium sulphate saturation at 4˚C, out of this xylanase activity was maximum at 70% ammonium sulphate fraction. The precipitated protein was dissolved in 0.1 M phosphate buffer (pH 6.8) and dialyzed. After ammonium sulphate precipitation and dialysis, the specific activity of enzyme increased 3.76 fold and 3.99 fold respectively.

3.3.2 Ion Exchange Chromatography

The elution profile of xylanase by using DEAE cellulose anion exchanger is shown in **Figure-2**. xylanase activity of each ion exchange chromatography fraction was determined as described previously, the enzyme activity and protein content was maximum in fraction number 8 and specific activity of that fraction reached 900 IU/mg. After ion exchange chromatography specific activity of partially purified enzyme increased 34.87 fold.

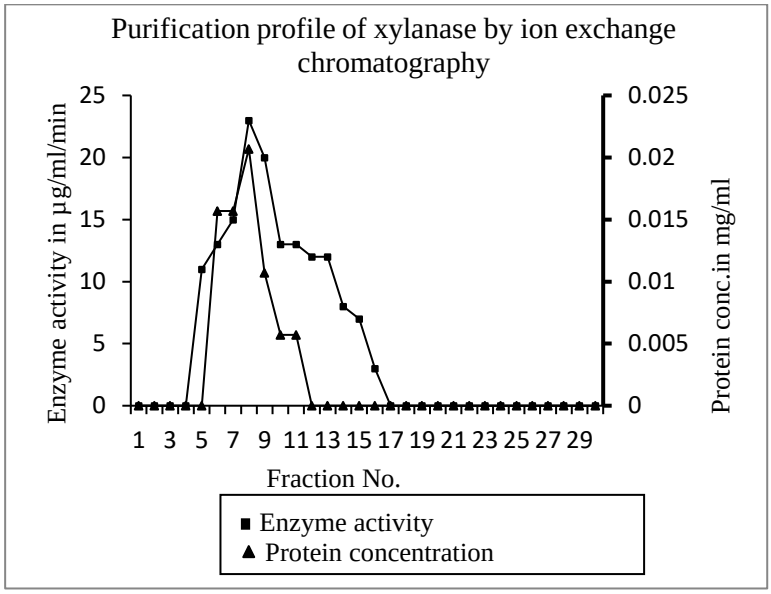

Figure-2. Purification profile of xylanase by ion exchange chromatography.

3.4 Optimization of enzyme

3.4.1 Effect of pH on enzyme activity

The purified enzyme activity was quantified in the pH range between 6.0 to 7.8. The enzyme activity was maximum at pH 6.8., below and above this pH enzyme activity was significantly lower (**Figure-3**).The graph shows that the xylanase production from *Cellulomonas flavigena* NCIM 2481 was highly depend on pH. After pH 7.0 xylanase activity was decreased, this might be due to the inhibitory effect of alkaline conditions on enzyme activity.

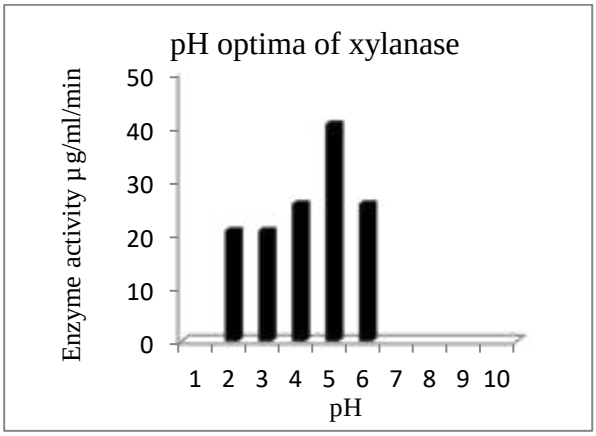

Figure-3. Effect of pH on enzyme activity.

3.4.2 Effect of temperature on enzyme activity

The xylanase activity was examined within the temperature range 20˚C to 80˚C, activity profile at different temperature is as shown in **Figure-4**. The enzyme activity increased up to temperature 50˚C and then declined progressively hence optimum temperature of xylanase was 50˚C. Above and below that temperature activity was decline considerably.

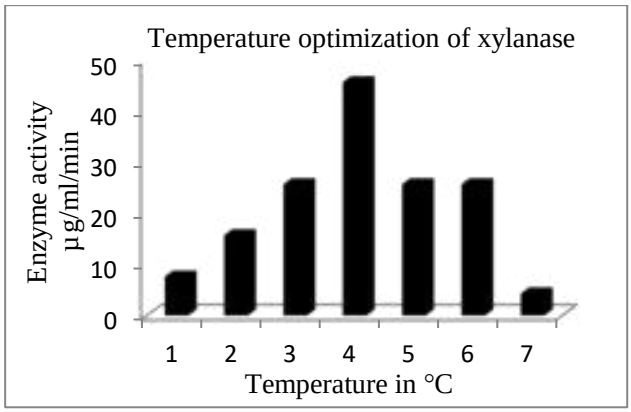

Figure-4. Effect of temperature on enzyme activity.

3.5 Km of xylanase

The kinetic parameter, Km of the enzyme was estimated by Lineweaver-burk plot of xylanase activity at 50°C using various concentrations of xylan as substrate. The Km value of xylanase isolated from *Cellulomonas flavigena* NCIM2481 was 2.78mg/ml hence enzyme has high affinity for the substrate. The range of km values of xylanases isolated from different sources was shown between 0.5 and 19.6 mg/ml [16]. The km estimated in this study was close to the km of xylanase isolated from *A. ficuum* AF 98 (3.267 mg/ml) [17].

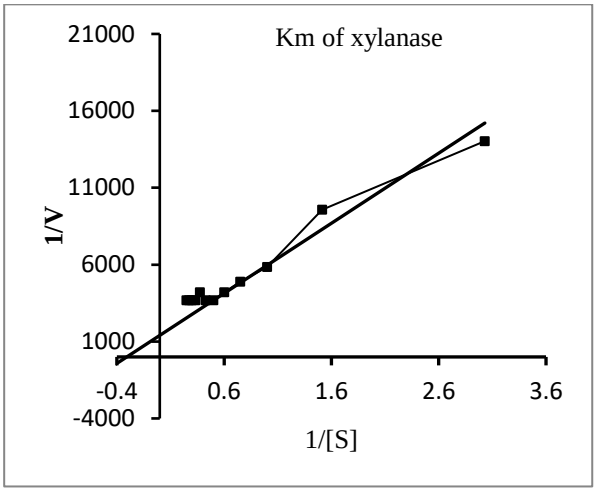

Figure-5. Effect of substrate concentration on enzyme activity.

Table-1. Purification steps of xylanase enzyme isolated from *Cellulomon as flavigena* NCIM 2481.

Purification steps	Activity µg/ml/min	Protein content In mg	Specific activity
Crude	40.6	1.473	25.81
Ammonium sulphate ppt.	16.83	0.173	97.28
Dialysis	17.83	0.173	103.06
Ion Exchange Chromatography	20.7	0.023	900

4. DISCUSSION

The xylanase producing *Cellulomonas flavigena* NCIM 2481 has given maximum activity of 40.6 U in 7th day of incubation on basal media at room temperature. This may suggest that the selected strain *Cellulomonas flavigena* NCIM 2481of the *Cellulomonas* sp. could serves as a significant practical explanation for the questions arising for maximal xylanase production and their various industrial applications. The optimum pH of xylanase was 6.8 and optimum temp was 50˚C which indicates the stain may be utilized for the enzyme production in even certain higher ranges of temperatures. After partial purification of xylanase up to ion exchange chromatography, the specific activity of enzyme increased 34.87 fold. The Km of xylanase was 2.78 mg xylan/ml, indicating high affinity of enzyme for the substrate. This detailed study will be more beneficial for the industrial production as well as enzymological studies.

REFERENCES

1. Subramaniyan, S., and Prema, P. (2002) Critical Reviews in Biotechnology, 22, 33-46.
2. Eduardo da Silva, A., Marcelino, H. R., Gomes, M. C. S., Oliveira, E. E., Nagashima, T., Egito, E. S. (2012) Intech Europe, 45, 61-84.
3. Mittal, A., Nagar, S., Kaur, K. S. J., Gupta, V. K. (2012) International Journal of Research and Development in Pharmacy and Life Sciences, 1, 63-68.
4. Li, X., She, Y., Sun, B., Song, H., Zhu, Y., Lv, Y., Song, H. (2010) Biochemical Engineering Journal, 52, 71–78.
5. Juturu, V., Wu, J. C. (2012) Biotechnology Advances, 30, 1219–1227.
6. Beg, Q., Kapoor, M., Mahajan, L., Hoondal, G. (2001) Applied Microbiology and Biotechnology, 56, 326–338.
7. Polizeli, M. L. T. M., Rizzatti, A. C. S., Monti, R., Terenzi, H. F., Jorge, J. A., Amorim, D. S. (2005) Applied Microbiology and Biotechnology, 67, 577–591.
8. Harris, A. D., Ramalingam, C. (2010) Journal of Experimental Sciences, 1, 01-11.
9. Kumar, L., Nagar, S., Kumar, D.,Garg, N., Gupta, V. K. (2013) International Journal of Cell Science and Biotechnology, 2, 1-10.
10. Wong, K. K., Tan, L. U., Saddler, J. N. (1988) Microbiological Reviews, 52, 305-317.
11. Riswan Ali, S. B. (2012) Asian Journal of Biochemical and Pharmaceutical Research, 2, 154-174.
12. Martínez-Trujillo, A., Pérez-Avalos, O., Ponce-Noyola, T. (2003) Enzyme and Microbial Technology, 32, 401–406.
13. Lowry, O. H., Rosebrough, N. J., Farr, A. L., Randall, R. J. (1951) Journal of Biological Chemistry, 193, 265.
14. Price, N. C. (1985) Biochemical Education, 13, 18.
15. Song, J. M., Wei, D. Z. (2010) Biomass Bioenergy, 34, 1930–1934.
16. Ghanem, N. B., Yusef, H. H., Mahrouse, H. K. (2000) Bioresource Technology, 73,113-121.
17. Lu, F., Lu, M., Lu, Z., Bie, X., Zhao, H., Wang, Y. (2008) Bioresource Technology, 99, 5938–5941.

Potential applications of phyto-components against Monosodium glutamate induced oxidative damage in *Saccharomyces cerevisiae* cells

Harshad K. Bote[a], Samidha S. Kakade[a], Neha K. Kamble[a], Anjali S. Kale[a], Sunita B. Kurane[a], Pankaj K. Pawar[a,*]

[a]Department of Biochemistry, Shivaji University, Kolhapur 416 004 (MS) India.

*Corresponding author: pkp.biochem@unishivaji.ac.in

ABSTRACT

The goal of the current study was to investigate the potential antioxidant properties of the plant-derived secondary metabolites Chebulinic acid (CA) and Boeravinone B (BB) in the presence of oxidative stress brought on by monosodium glutamate (MSG), tartazine, and sunset yellow. Saccharomyces cerevisiae cells were treated with different concentrations MSG, Tartazine and Sunset yellow (1.0 – 40 µg/mL) and incubated up to 3 hrs to analyze Reactive Oxygen Species (ROS) production. MSG showed highest ROS levels at 2 hrs incubation so it was selected for further studies. In addition, the ability of ROS to be scavenged, the status of antioxidant enzyme activities (SOD, GPx, and CAT), the content of protein carbonyls (PCO), and the levels of lipid peroxides (LPO) were assessed following treatment with CA and BB. S. cerevisiae cells exposed to the oxidative stress caused by MSG are demonstrated to be extremely well protected by CA and BB. Additionally, compared to cells solely exposed to MSG, cells treated with CA and BB showed reduced levels of PCO and LPO content. It appears that the investigated phyto-compounds CA and BB are powerful natural antioxidants that can be employed to combat oxidative stress-related damage and severe diseases.

KEYWORDS

Oxidative stress, Monosodium glutamate, Antioxidants, Chebulinic acid, Boeravinone.

…….

1. INTRODUCTION

Food is a remarkably general source of toxicant exposure to human beings. Due to the tremendous rise in the working class and urbanization, commercial food consumption has a significant influence on the life-support system of the urban people today. People often eat commercial meals because they save time and energy, however these foods also often include a variety of food additives in them. More than 2500 chemical substances of various characteristics are used as food additives to improve flavor, color, stability, nutritive value and texture of food products. Food additives are the substances which are not generally been used as food. Sometimes

addition of low value or impure food additives leads to adulteration in food. This excessive consumption of adultered food have potential toxic effects on consumers health [1].

Earlier reports demonstrated that extensive use of sunset yellow and tartrazine causes arrest in G2/M growth phase, increased nuclear damage and increased percentage of apoptosis in kidney cells of chick embryo [2]. One of the ingredients that cuisine uses the most commonly is monosodium glutamate (MSG). Multiple reports have exposed that excessive use of MSG has deleterious effects on development of adults, adolescents, children and fetus [3]. An excess of reactive oxygen species (ROS) are produced when Sunset yellow, tartrazine, and MSG are administered, and this accelerates the apoptotic process, according to prior research in animal models [4,5].

ROS are highly reactive metabolic products which effects on physiological redox status and apoptotic processes in stressed cells. These ROS induce oxidative stress, macromolecular toxicity, mitochondrial dysfunction and inflammation in toxicant/adulterant exposed cells [6]. Multiple sclerosis, Parkinson's disease, Alzheimer's disease, diabetic kidney disease, and development of fatty liver disease are only a few examples of the metabolic illnesses that can occur from vigorous ROS formation over time, failure in organelles, and basic biological processes [7].

Considering these hazardous effects, there is need to develop potential strategy to conquer the ROS induced toxicities. Excessive generation of ROS could be controlled by lowering the exposure to toxicants or by increasing the amount of endo- and exo- genous anti-oxidants. As a result, the use of antioxidants can help to maintain a biological process at its best by removing too many free radicals. Previously researchers have used various plant extracts and secondary metabolites to control/reduce the ROS induced toxicities. Various plant extracts showed potential clinical and pharmacological activity to conquer ROS toxicities with less/no side effects [8]. In addition to this, ayurvedic polyherbal formulations were also used effectively to reduced diabetic complications any many other disorders in rats [9]. Recently, researchers have developed a great interest in the use plant secondary metabolites, which are safe, natural, potent antioxidant molecules; act through various mechanisms like ROS elimination, ions chelation, lipid peroxide elimination and inhibition of protein carbonylation.

Earlier, our group demonstrated potential role of CA and BB against various damages induced by industrial dye Malachite green [10]. Hence, the purpose of the present study is to screen different food additives for their toxicities and use of plant secondary metabolites Chebulinic acid and Boeravinone B to conquer the toxicities induced by these additives on cellular model system *Saccharomyces cerevisiae*.

2. EXPERIMENTAL SECTION

2.1. Chemicals

Dextrose anhydrous (GRM077), peptone type-III bacteriological (RM7709), yeast extract powder (RM668), agar powder (GRM026), L-Ascorbic acid (CMS1014) and Monosodium glutamate (TC561U) were acquired from Hi-Media Laboratory Products (India). Sunset Yellow FCF (68775), Tartrazine (03322), Griess reagent (G4410) and 2′,7′-Dichlorofluorescein diacetate (D6883) were obtained from Sigma Aldrich, India. Natural Remedies Pvt Ltd (India) provided the phyto-molecules, Chebulinic acid and Boeravinone B. All other chemical substances and solvents used for experimental work were of analytical grade and the highest purity available.

2.2. Culture growth conditions and experimental setup

The yeast strain *S. cerevisiae* (NCIM-3594) was purchased from the NCIM Research Center, Pune (India). The cell culture was maintained on 3% agar slants containing yeast extract (2%), peptone (2%), and dextrose (4%). Cells used for the current study were continuously grown on minutely amended culture media consisting of dextrose (2%), peptone (0.5%) and yeast extract (0.5%). For the entire study, five experimental sets were designed as a) a control set with untreated *S. cerevisiae* cells; b) MSG set with MSG (20 µg/mL)-exposed cells; c) MSG+ vit-C set with MSG-exposed cells treated with 5 µg/mL vit-C; d) MSG+CA set with MSG-exposed cells treated with 5 µg/mL CA; and e) MSG+BB set with MSG-exposed cells treated with 3 µg/mL BB. Cells used in the experimental setup were allowed to grow at 35 ± 2 °C in modified liquid media with continuous shaking at 110–130 rpm.

2.3. Determination of endogenous ROS levels in presence of Tartrazine, Sunset yellow and MSG

S. cerevisiae cells were treated with different concentration (1, 5, 10, 20 and 40 µg/mL) of Tartrazine, Sunset yellow and MSG for assessment of ROS generation by these additives, cells from all the sample sets were collected at 4-time breaks (0, 1, 2 and 3 hr, respectively) by centrifugation at 3000 rpm for 2 min in 2 mL aliquots. Collected cells were washed twice with 1 mL of 50mM phosphate buffer (pH 7.4) and re-suspended in 2 ml same buffer. To this cell suspension, 1mM ethanolic stock solution of 2′,7′-Dichlorofluorescein diacetate (H_2DCF-DA) was added to attain 10µM final concentration of the H_2DCF-DA dye. After treatment of dye suspension was incubated in dark at 28° C for 20 mins. Then, cell suspension was centrifuged at 3000 rpm for 2 mins and clarified. The fluorescence of supernatant was measured (excitation at 488nm and emission at 520nm for each sample) using spectrofluorometer and expressed as relative fluorescence units/mL of protein extract.

2.4. Alteration in endogenous ROS levels after treatment of CA and BB

2’7’- Dichlorofluorescin diacetate (H_2DCF-DA) was used to ascertain subcellular ROS levels. This dye has chemical characteristic feature due to which it enters through cellular membrane and react with oxidants (ROS) present in the cell. H_2DCF get oxidized by ROS and shows fluorescence, which is quantified spectrofluorometrically. *S. cerevisiae* cells were augmented with MSG (20 µg/mL) and treated with CA and BB as mentioned in experimental setup. For assessment of ROS generation by MSG and ROS scavenging potential of CA and BB, cells from all the sample sets were collected after 2 hr of incubation by centrifugation. Collected cells were treated and incubated with H_2DCF dye as mentioned above and the fluorescence was measured (excitation at 488nm and emission at 520nm for each sample) using spectrofluorometer [11].

2.5. Nitrite estimation by Griess method

For exogenous nitrite estimation, 2 mL media from all experimental sets was taken and centrifuged at 8000 rpm for 5 mins. Supernatant was used as cell free media to estimate exogenous nitrite content. 200 µL cell free media was mixed with 200 µL Griess reagent and incubated for 20 mins in dark at ambient temperature. Extracellular nitrite content was quantified spectrophotometrically at 430 nm and nitrite formation due to MSG-induced stress was calculated using sodium nitrite as standard [12].

2.6. Preparation of crude cell free extract

S. cerevisiae cells (2 mL) from each mentioned experiment sets were washed twice with phosphate buffer (50 mM, pH 7.4) and then resuspended in 1 mL chilled phosphate buffer (50 mM, pH 7.4). Cells were then homogenized using a homogenizer and then sonicated with output at 60 amp, giving three strokes each of 45 s, followed by 2 mins cooling on ice. The homogenate obtained was centrifuged (12000 rpm, 10 mins, 40 °C). The supernatant was used as crude cell free cytosolic extract for further experiments. Total protein content was calculated by Bradford’s estimation method [13].

2.7. Enzyme activity assays of SOD, GPx and CAT

MSG accumulation causes vigorous generation of superoxide radicals. The capacity of crude cytosolic extract to prevent NADH from being oxidised by ROS produced in chemical systems was evaluated in order to measure SOD activity.For this analysis a reaction mixture comprising 10 mM EDTA, 2.5 mM MgCl2, 130 mM methionine, 150 mM NBT and 60 M riboflavin was added to 100 µL of crude enzyme extract that had been prepared in 50 mM potassium phosphate buffer at a pH of 7.4. A 560 nm wavelength was used to analyze the kinetics of the SOD enzyme [14].

The CAT enzyme activity was estimated by calculating Hydrogen peroxide (H_2O_2) utilization by crude cytosolic extract from each set. The reaction mixture

contained 30% H_2O_2 in 100 mM potassium phosphate buffer (pH 7.0) and 100 µL of the enzyme extract. The enzyme kinetic progress was assessed at 240 nm wavelength. The CAT activity was expressed as nmol H_2O_2 utilization/min/mL of lysate [15].

The GPx assay is coupled assay with Glutathione reductase (GR). The GPx activity was determined based on monitoring at 340 nm decrease in absorbance due to the oxidation of secondary substrate NADPH by Glutathione reductase (GR). The assay recording of NADPH oxidation measures the H_2O_2 reduction by GPx to alcohol. For this purpose, a reaction mixture containing assay buffer (50 mM Tris HCl containing 0.5 mM EDTA), NADPH assay reagent (5 mM NADPH, 42 mM reduced glutathione and 10 U/mL Glutathione reductase), and tert-butyl hydroperoxide(luperox) with 50 µL of enzyme extract was used. The kinetics of the activity was measured at a wavelength of 340 nm. The unit of the activity was expressed as µmol NADPH oxidized per min per mL of lysate [16].

2.8. Estimation of total protein carbonyl content by the DNPH method

The assessment of total carbonyl content was done as per Levine's method. Briefly, 400 µL of the crude cytosolic extract from each set was combined with 400 L of 2,4-dinitrophenylhydrazine (DNPH) at a concentration of 10 mM, and the mixture was then let to sit at room temperature for 45 minutes. Then, proteins were precipitated using 500 µL of chilled 20 percent (w/v) trichloroacetic acid (TCA), maintained on ice for 10 minutes, and centrifuged at 12,000 g for 10 minutes at 4 °C. The protein pellet was collected and subjected to two washes in a 750 µL acetone solution. After that, the protein sample was resuspended in 400 µL of 6 M guanidine-HCl, and samples' absorbance was read at a wavelength of 370 nm. In crude cytosolic extract, the total protein carbonyl concentration was shown as nmol/mg of protein [17].

2.9. Anti-lipid peroxidation assay

The potential of CA and BB to stop the production of malondialdehyde (MDA) was used to evaluate the anti-lipid peroxidation potential. For this 400 µL crude cytosolic extract from each set was perfused in 400 µL of 0.15 M ice-cold KCl. The reaction mixture was then given 750 µL of a 0.4 percent TBA and 15 percent TCA solution made in 0.25 M hydrochloric acid. The reaction mixture was promptly cooled after being boiled in a boiling water bath for 15 minutes. The reaction mixture was then mixed with 500 µL of n-butanol and centrifuged at 8,000 g for five minutes. At a wavelength of 532 nm, the absorbance of the supernatant's top layer was measured, and the findings were reported as nmoles MDA/mg of protein [18].

2.10. Statistical analysis

Results for three experiments ($n \geqslant 3$) were represented as means standard deviation (± SD) for each experiment that was done in triplicate. One-way ANOVA was used

to express the statistical significance of the variance [19]. P value, $P \leqslant 0.05$ or 0.01 was used to determine significance.

3. RESULTS AND DISCUSSION

In *S. cerevisiae* cells under MSG stress, excessive ROS production can outpace the capability of the cell's principal antioxidant defence system, which over time causes oxidative damage to numerous cellular components and ultimately leads to the emergence of various oxidative stress-related diseases. Therefore, external supplementation of natural antioxidants could help to conquer free radical holocaust and to hold an ideal biological system by scavenging excessive free radicals. Hence, the target of this work was to investigate the efficacy of CA and BB treatments against MSG-induced oxidative damage in *S. cerevisiae* cells. Here, we have screened different food additives for their oxidative stress inducing potential and out of which we have selected MSG as potential stress inducer. Then, we have assessed ROS scavenging potential, anti-oxidant enzyme status, protein carbonyl content and lipid peroxide concentrations in CA and BB treated *S. cerevisiae* cells.

3.1. Alteration in endogenous ROS levels after treatment of CA and BB

The damage caused by MSG induced stress in *S. cerevisiae* have been linked with an elevated ROS level, alteration in enzyme activity and collapsed mitochondrial functioning. Intracellular ROS was estimated using fluorescent ROS indicator H_2DCFDA. First, ROS generation in Tartrazine, Sunset yellow and MSG was investigated using different concentrations (1, 5, 10, 20 and 40 μg/mL) of these additives at various time intervals (0, 1, 2 and 3 hr). Up to two hours after incubation, all three additions increased the levels of ROS, with MSG exhibiting greater ROS levels than Tartrazine and Sunset yellow (**Figure-1**). Then, we selected MSG (20 μg/mL) for further investigations and determined change in ROS generation after CA and BB treatment at 2 hr incubation. We found that CA and BB treatments lowered the ROS generation by 42.03 and 66.56 % respectively, as compared to MSG-exposed cells (**Figure-2a**). Interestingly, reduction in ROS levels after CA and BB treatment suggest their potential ROS scavenging ability in MSG-exposed *S. cerevisiae* cells.

The damage caused by MSG induced stress in *S. cerevisiae* have been linked with an elevated ROS level, alteration in enzyme activity and collapsed mitochondrial functioning. Intracellular ROS was estimated using fluorescent ROS indicator H_2DCFDA. First, ROS generation in Tartrazine, Sunset yellow and MSG was investigated using different concentrations (1, 5, 10, 20 and 40 μg/mL) of these additives at various time intervals (0, 1, 2 and 3 hr). Up to two hours after incubation, all three additions increased the levels of ROS, with MSG exhibiting greater ROS levels than Tartrazine and Sunset yellow (**Figure-1**). Then, we selected MSG (20 μg/mL) for further investigations and determined change in ROS generation after CA and BB treatment at 2 hr incubation. We found that CA and BB treatments lowered

the ROS generation by 42.03 and 66.56 % respectively, as compared to MSG-exposed cells (**Figure-2a**). Interestingly, reduction in ROS levels after CA and BB treatment suggest their potential ROS scavenging ability in MSG-exposed *S. cerevisiae* cells.

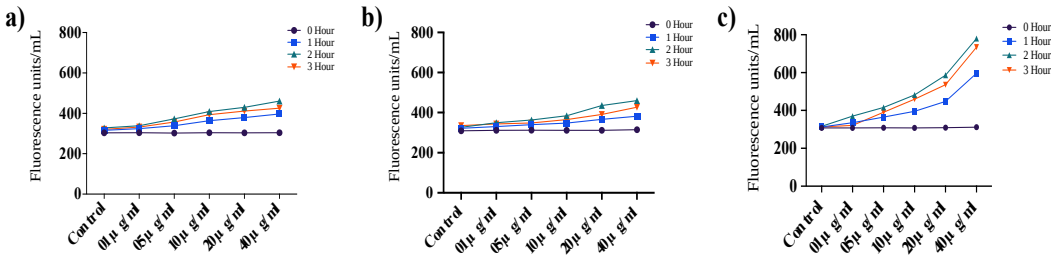

Figure-1. Determination of endogenous ROS levels in presence of a) Tartrazine, b) Sunset yellow and c) Monosodium glutamate (MSG). Experimental data is presented as the mean ±SD of the three corresponding experimental sets (n=3). CV and p values of the treatment sets substantially differed from those of the MG set (*p≤0.03; CV≤0.05).

3.2. Nitrite estimation by Griess method

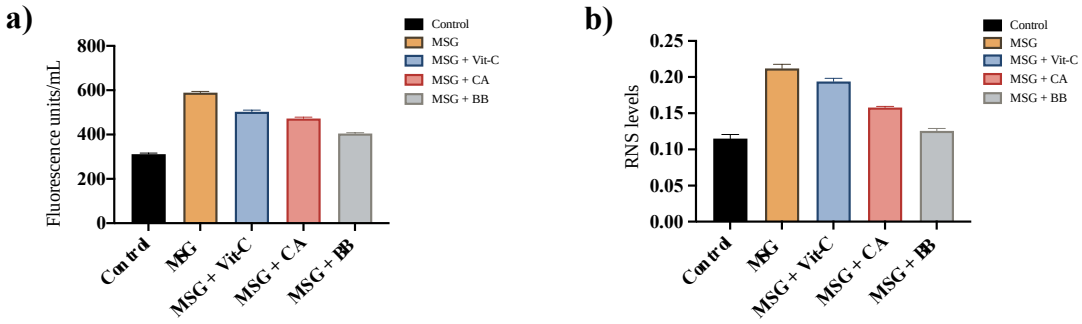

Figure-2. Biochemical assays for a) Estimation of endogenous ROS levels after treatment of CA and BB b) Estimation of nitrite content by Griess method. Experimental data is presented as the mean ±SD of the three corresponding experimental sets (n=3). CV and p values of the treatment sets substantially differed from those of the MG set (*p≤0.03; CV≤0.05).

Griess assay was carried out for relative quantification of the nitrite formation in all the treatment sets. After a 20 min incubation in cell-free culture media, CA and BB treatments showed lowered RNS generation by 55.67 and 89.69 % respectively, as compared to MSG-exposed cells (**Figure-2b**). This observation suggests that the

change in kinetics of RNS liberation is an important factor for the neutralization of MSG induced cytotoxicity after CA and BB treatment.

3.3. Activity of antioxidant enzymes (SOD, GPx and CAT)

Eukaryotic cells possess evolutionarily conserved systems to regulate the production of ROS and safeguard cells from their oxidative damage. One of which is primary antioxidant defense system, consists of antioxidant enzymes CAT, SOD and GPx. Hence, we have assessed enzyme activities of SOD, GPx and CAT in all experiment setups.

We found that SOD activity in MSG-stressed cells got elevated up to 0.265 nmol/min/mL as compared to control cells (0.140 nmol/min/mL), which was then lower by CA and BB treatments to 0.237 nmol/min/mL and 0.185 nmol/min/mL, respectively (**Figure-3a**). Similarly, GPx activity in MSG-stressed cells got elevated up to 0.360 µmol/min/mL as compared to control cells (0.025 µmol/min/mL), which was then lower by CA and BB treatments to 0.190 and 0.105 µmol/min/mL, respectively (**Figure-3b**). Further, the CAT activity in MSG-stressed cells got elevated up to 5.430 nmol/min/mL as compared to control cells (0.245 nmol/min/mL), which was then lower by CA and BB treatments to 1.350 nmol/min/mL and 0.740 nmol/min/mL, respectively (**Figure-3c**). Thus, decreased activities of antioxidant defense enzymes (SOD, GPx and CAT) after CA and BB treatments suggest the ROS scavenging potential of CA and BB molecules.

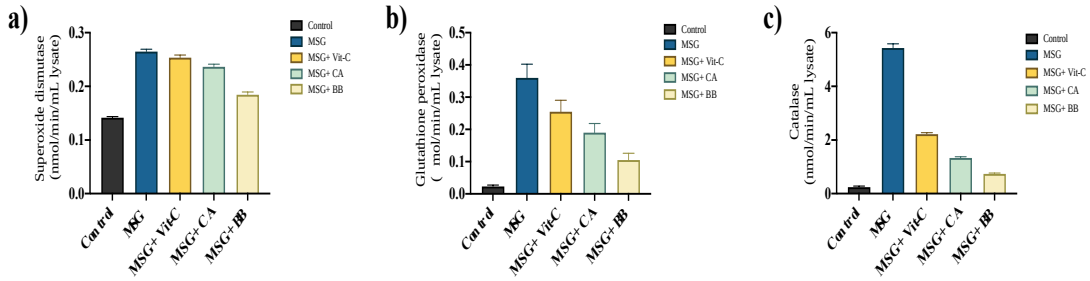

Figure-3. Enzyme activity assays of a) SOD, b) GPx and c) CAT. Experimental data is presented as the mean ±SD of the three corresponding experimental sets (n=3). CV and p values of the treatment sets substantially differed from those of the MG set (*p≤0.03; CV≤0.05).

3.4. Protein carbonyl content

Protein carbonylation is one of macromolecular damage linked with oxidative stress. Oxidative modifications of certain amino acids or breakage of peptides lead to

formation of protein carbonyls, this is irreversible process and stated as one of the major proteins damaging process. The DNPH method is used for measurement of total protein carbonyl content related to oxidative damage [20].

Results demonstrated that the protein carbonyl content was higher by 1.95-fold (0.718 nmol/mL of lysate) in MSG- exposed cells, as compared to the control set (0.746 nmol/mL of lysate). CA and BB treatments reduced protein carbonyl content to 1.42-fold (1.063 nmol/mL of lysate) and 1.41-fold (1.055 nmol/mL of lysate), respectively. compared to MSG-exposed cells (**Figure-4a**). In our findings, Comparing the MSG-exposed cells to the control sample, the protein carbonyl level was noticeably greater. Treatment with CA and BB stabilises the protein against oxidation and shows a considerable guarding capacity against oxidative damage.

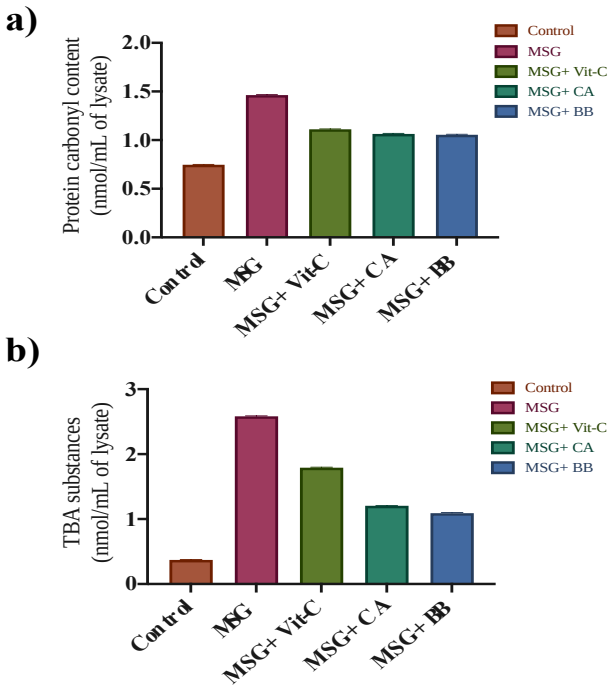

Figure-4. Biochemical assays for a) Estimation of total protein carbonyl content by the DNPH method b) Estimation of TBA substances. Experimental data is presented as the mean ±SD of the three corresponding experimental sets (n=3). CV and p values of the treatment sets substantially differed from those of the MG set (*p≤0.03; CV≤0.05).

3.5. Anti-lipid peroxidation

MSG exposure leads to vigorous generation of ROS. These ROS get reacted with polyunsaturated fatty acids (PUFA) to generate malondialdehyde (MDA). MDA can

eventually serve to ascertain the concentration of lipid peroxides formed in cells [20]. In present investigation levels of TBA-MDA adducts were used to determine the damage to lipids. Here, TBA-MDA adducts formed were considered 100% and 0% in in MSG-exposed and control set, respectively. Assuming this, CA and BB treatments showed decrease in MDA adduct levels by 53.33 and 57.75 % respectively, as compared to MSG-exposed cells (**Figure-4b**). Decrease in TBA-MDA levels shows inhibition in lipid peroxide formation and suggest the anti-lipid peroxidation (ALPO) potential of CA and BB in MSG-exposed cells. MSG induced oxidative stress is associated with damage to various micro-molecules, macromolecules and organelles, which can be conquered by CA and BB molecules [21].

4. CONCLUSION

In light of above experimental information, we can conclude that the ROS and oxidative damage induced by MSG in *S. cerevisiae* cells was exhibited in various different forms like increased antioxidant enzymes activity, protein carbonylation, MDA levels and impairment of cellular elements. Additionally, the natural antioxidants CA and BB showed a guarding effect against oxidative stress and related damages in *S. cerevisiae* cells. After administering CA and BB to the MSG-stressed cells, the activity of antioxidant defence enzymes (SOD, GPX, and CAT) was eventually restored to normal levels, and the therapy also decreased the levels of protein carbonyls and MDA. In conclusion, more study on these phyto-components, which have the potential to be very effective in defending organisms against the significant illnesses and damages brought on by oxidative stress, might be done.

ACKNOWLEDGEMENT

The authors particularly express gratitude for DST-FIST, UGC, New Delhi for their financial support through the SAP-DRS-Phase-II grant. Among the authors listed, H. Bote is grateful to UGC New Delhi for awarding the UGC-Junior Research Fellowship.

REFERENCES

1. Pressman, P., Clemens, R., Hayes, W., Reddy, C. (2017) Toxicology Research and Application, 1, 1-22.
2. El-Borm, H. T., Badawy, G. M., Hassab El-Nabi, S., El-Sherif, W. A., Atallah, M. N. (2020) Egyptian Journal of Zoology, 74, 43-55.
3. Chakraborty, S. P. (2019) Toxicology Mechanisms and Methods, 29, 389-396.
4. Khayyat, L. I., Essawy, A. E., Sorour, J. M., Soffar, A. (2018) Peer Journal, 6, 5689.

5. El-Borm, H., Badawy, G. M., El-Nabi, S. H., El-Sherif, W., Atallah, M. (2019) European Journal of Pharmaceutical and Medical Research, 6, 48-64.
6. Alfadda, A. A., Sallam, R. M. (2012) Journal of Biotechnology and Biomedicine, 97, 65-67.
7. Johnson, J., Mercado-Ayon, E., Mercado-Ayon, Y., Dong, Y. N., Halawani, S., Ngaba, L., Lynch, D. R. (2021) Archives of Biochemistry and Biophysics, 702, 108698.
8. Gupta, V. K., Sharma, S. K. (2006) Natural Product Radiance, 5, 326-334.
9. Renganathan, S., Pillai, R. G. (2020) Journal of Diabetes and Metabolic Disorders, 19, 1345-1355.
10. Biradar, S. P., Tamboli, A. S., Khandare, R. V., Pawar, P. K. (2019) Mitochondrion, 46, 236-246.
11. Sj, S., Veerabhadrappa, B., Subramaniyan, S., Dyavaiah, M. (2019) FEMS Yeast Research, 19, 113.
12. Griess, J. P. (1864) Philosophical Transactions of the Royal Society B, 154, 667-731.
13. Bradford, M. M. (1976) Analytical Biochemistry, 72, 248-254.
14. Weydert, C. J., Cullen, J. J. (2010) Nature Protocols, 5, 51-66.
15. Gamero-Sandemetrio, E., Gómez-Pastor, R., Matallana, E. (2014) Biotechnology Journal, 9, 1055-1064.
16. Ridaoui, K., Guenaou, I., Taouam, I., Cherki, M., Bourhim, N., Elamrani, A., Kabine, M. (2022) Saudi Journal of Biological Sciences, 29, 1842-1852.
17. Levine, R. L. (2002) Free Radical Biology and Medicine, 32, 790-796.
18. Samokyszyn, V. M., Marnett, L. J. (1990) Free Radical Biology and Medicine, 8, 491-496.
19. Ross, A., Willson, V. L. In One-way anova, edited by Ross, A. Springer, (2017) pp.21-24.
20. Fedorova, M., Bollineni, R. C., Hoffmann, R. (2014) Mass Spectrometry Reviews, 33, 79-97.
21. Jia, R., Li, Y., Cao, L., Du, J., Zheng, T., Qian, H., Yin, G. (2019) Comparative Biochemistry and Physiology C, 215, 56-66.

Biodegradation of lignin sulfonic acid sodium salt from Rhodococcus NCIM 2891

Naiem H. Nadaf[a*], Shailesh R.Waghmare[a], Pradeep M. Gurao[b], Nitin M. Naik[a,*]
[a]Department of Microbiology, Shivaji University, Kolhapur 416 004 (MS) India.
[b]Department of Biochemistry, Shivaji University, Kolhapur 416 004 (MS) India.
*Corresponding author: nhnadaf@gmail.com

ABSTRACT
Rhodococcus sp. NCIM 2891 was cultivated in minimal medium supplemented with lignin sulfonic acid sodium salt 1gm L^{-1} concentration. It was observed that the microorganism was capable to hydrolyze lignin sulfonic acid sodium salt within 15 days of incubation however the first step is desulfonation of lignin sulphonic acid. The degradation of lignin sulfonic acid sodium salt was determined by the analytical techniques like, UV-visible Spectrophotometer FTIR GC-MS. The enzyme profiles were investigated during the course of degradation the studied enzymes are Lignin peroxidase 8.4 U/mg of protein; polyphenol oxidase 31.42U/mg of protein, catechol oxidase 32.5 U/mg of protein, tyrosinase18.8U/mg of protein and catechol 1, 2-dioxygenase 64U/mg of protein. The SDS-PAGE analysis revealed that the purified enzymes has molecular weights as catechol 1, 2 dioxygenase about 30kD tyrosinase - 36kD, polyphenol oxidase - 50kD, and catechol oxidase -30kD respectively.

KEYWORDS
Rhodococcus, Sulfonates, Polyphenol oxidases, Degradation, Catechol, Lignin.

…….

1. INTRODUCTION

Industrial effluents derived from wood pulping, chlorine-bleaching processes contain a wide range of aromatic compounds that can include lignin, degraded products of lignin, and modified products such as lignosulfonates are highly resistant to biodegradation by most microorganisms [1,2]. Lignin is the second most abundant plant cell wall biopolymer, comprising 15% of the Earth's biomass [3] it is a heterogeneous structure consisting of phenyl-propanoid units and the principal source for aromatic compounds found [4,5] and consists of an apparently random complex of phenolic and non-phenolic compounds [6]. Because of the bond types and their heterogeneity, lignin and lignin related compounds like lignosulfonates cannot be cleaved by hydrolytic enzymes as most other natural polymers [7].

Conventional methods for the treatment of these phenolic wastes have been mostly physicochemical, but since they cause secondary pollution problems in the environment, biological treatments are preferred for large-scale removal of this type

of pollutants [8]. Conversion of lignosulfonates into low molecular substances is probably an effective way to increase their utility. Lignins have been successfully degraded into phenols, low molecular weight acids, and the degradation products can be used as fuels, chemical products, or feedstock in the manufacture of polymeric materials [9,10].

Furthermore, the breakdown products of these phenolic compounds may be more harmful when these compounds are incompletely degraded by physical and chemical methods or natural oxidation. Therefore, the optimum removal and consumption of these substances from industrial and domestic water bodies is of great importance in point of view of environmental protection [11].

The genus *Rhodococcus* is comprised of genetically and physiologically diverse bacteria, which have been isolated from various habitats like soil and seawater. Since they are involved with a large number of enzymatic activities, unique cell wall structure and suitable biotechnological properties, *Rhodococcus* strains may be utilized as industrial organisms, primarily for biotransformation and the biodegradation of many organic compounds [12]. However, the *Rhodococcus* NCIM 2891 and other strains of *Rhodococcus* are used for the desulfurization and desulfonation studies of the petrochemicals to obtain the sulfur free petroleum sources.

In this context, the study deals with utilization of lignin sulfonic acid sodium salt as a sole of carbon for the *Rhodococcus* NCIM 2891. It involved the study of degradation and modification of lignin sulphonic acid, by *Rhodococcus* NCIM 2891 and study of enzyme like phenol oxidases and peroxidases, production during the course of degradation.

2. EXPERIMENTAL SECTION

2.1. Microorganism

Rhodococcus NCIM 2891 was obtained from NCIM (National Collection of Industrial Microorganisms), India. The culture was maintained on YEME (Glucose Yeast extract Malt extract) agar having the following composition 1% glucose, 0.3 % yeast extract, 0.3 % malt extract 0.5% peptone and 1.5 % bacteriological agar for solidification.

2.2. Growth of bacteria on lignin sulfonic acid sodium salt

The lignin sulfonic acid sodium salt utilizing *Rhodococcus* NCIM 2891 was grown by inoculating a 5 mL of 18 hrs old culture cells grown in YEME liquid medium and used as an inoculum. This culture had a cell density of 3 x 10^8/mL, was added aseptically in flask containing medium (0.3% Na_2NO_3, 0.1% K_2HPO_4, 0.05% $MgSO_4$, 0.05%KCL, 0.0001% $FeSO_4$, 0.05%, yeast extract and 0.1% lignin

sulphonic acid sodium salt and pH adjusted to 7.0) was incubated in shaking condition (120 rpm) at 25^{o}C under aerobic condition. The experiment was carried out in triplicates. The degradation of lignin sulfonic acid sodium salt was monitored every 5 days, by processes as described below.

2.3. Analysis of degraded product

2.3.1. UV – visible analysis for lignin degradation

The cell free medium obtained after centrifugation of incubated medium at 6400 g. This was analyzed for its absorption maximum against uninoculated medium as control. Samples were diluted 10^2 times with the same sterile medium before analysis and analysis were carried out spectrophotometrically using a Hitachi U-2800 spectrophotometer.

2.3.2. Fourier transform infrared spectroscopy (FTIR)

The cell free medium which was obtained after 10 and 15 days of incubation were taken and dried in oven at 40^{o}C, the dry powder samples were analyzed by FTIR in the mid IR region of 400-4000 cm^{-1} with 16 scan speed. The pellets prepared using spectroscopic pure KBr (5:95).

2.3.3. Gas chromatography-Mass spectroscopy (GC-MS)

The cell free medium and diethyl ether was mixed in 1:1 proportion and then the ether layer was evaporated and redissolved in acetonitrile. This solution was then analyzed by GC-MS, using a QP 5000 mass spectrophotometer (Shimadzu). The ionization voltage was 70 eV. Gas chromatography was conducted in temperature programming mode with a Resteck column (0.25 mm × 30 mm; XTI-5). The initial column temperature was 40 °C for 4 min, then increased linearly at 11 °C min^{-1} to 300 °C and held at 29 min. The temperature of injection port was 275 °C and GC-MS interface was maintained at 300 °C. Helium was used as carrier gas with flow rate 1 ml min^{-1} and 30 min run time.

2.4. Purification of enzymes

After 10 days of incubation, cells were harvested by centrifugation at 6400 x g, for 20 minutes. The harvested cells were washed twice with 30 ml of 50 mM sodium phosphate buffer (pH = 7.0) and resuspended in the same buffer and used for the extraction of catechol 1, 2-dioxygenase. The remaining cell free medium was used for the isolation and extraction of extracellular enzymes like, polyphenol oxidase, catechol oxidase, tyrosinase and partial purification of lignin peroxides separately.

2.4.1. Purification of catechol 1, 2-dioxygenase

The harvested cells were homogenized by sonication with vibra model VC.130PB sonicator at 50 amplitude for 5 mins and centrifuged for 30 mins at 8900 x g. The

supernatant was then subjected for the ammonium sulphate precipitation at 80 % saturation and the precipitate obtained was redissolved in 10 ml of 50 mM sodium phosphate buffer (pH = 7.0). In next step of purification, the enzyme extracts were subjected to DEAE - Cellulose ion exchange column chromatography. The column was eluted with 50 fractions of a step gradient of NaCl with concentration from 0 to 0.2 M in 50 mM sodium phosphate buffer (pH 7.0) at a flow rate of 0.5 ml min^{-1}. The protein concentrations of eluted fractions were analyzed by taking absorbance at 280 nm. The fractions with protein were tested for Catechol 1, 2-dioxygenase activities. The fractions containing Catechol 1, 2-dioxygenase activities were used for SDS/PAGE analysis.

2.4.2. Purification of Extracellular phenol oxidases

The enzymes, tyrosinase, polyphenol oxidase, catechol oxidase and lignin peroxidase were purified from cell free medium. The cell free medium was taken and subjected for ammonium sulphate precipitation at 80 % saturation. The precipitate obtained was redissolved in 20 ml of 50 mM sodium phosphate buffer (pH = 7.0). This was then further purified by DEAE - Cellulose ion exchange chromatography. The protocol for Ion Exchange Chromatography is similar to that of used for the purification of catechol 1, 2-dioxygenase enzyme.

2.4.3. SDS/PAGE analysis of enzyme

The molecular weights of enzymes were determined by the SDS/PAGE [13]. The analysis of molecular weight of purified enzyme were carried out by using protein molecular weight markers that are phosphorylase b (97.4 kDa), Bovine Serum albumin (66 kDa), ovalbumin (43kDa), carbonic anhydrase (29 kDa), trypsin inhibitor (20.1 kDa), and lactabumin (14.3 kDa).

2.5. Enzyme assays

2.5.1. Catechol 1, 2 dioxygenase

Catechol 1, 2-dioxygenase activity was assayed spectrophotometrically [14] using a Hitachi U-2000 spectrophotometer. The standard assay of enzyme activity was performed by making an assay mixture containing 5 µl of Catechol 1, 2-dioxygenase, 20 µl of 10 mM Catechol as a substrate and final volume adjusted to1 ml with 50mM sodium phosphate buffer (pH 7.0). The enzyme activity was monitored by measuring the formation of cis, cis-muconic acid at A 265_{nm} (ε = 16.8 mM). One unit of the enzyme activity was defined as the amount of the enzyme required for the formation of 1 µmol of cis, cis-muconic acid per min at 25°C.

2.5.2. Catechol oxidase

The enzyme assay of catechol oxidase was carried out with spectrophotometrically by using 5mM catechol as a substrate. The reaction mixture contains 2.80 ml buffer,

0.10 ml 5 mM Catechol, 0.10 ml 2.1mM Ascorbic acid and 0.10 ml enzyme solution against blank that contain same reaction mixture accept enzyme and ascorbic acid. One unit activity will cause the change in A 265 $_{nm}$ of 0.001 per minute at pH 7and at 25°C in 3 ml reaction mixture containing catechol and ascorbic acid [15].

2.5.3. Lignin peroxides

Lignin peroxidase activity of the culture supernatant was assayed using 2, 4 dichlorophenol assay based on the reaction of lignin peroxidase oxidized 2, 4 diclorophenol with 4 – aminoantipyrine to form a coloured antipyrylquinonimine that strongly absorbs at A 510 $_{nm}$. The final concentration of the 1 mL aqueous assay mixture consists of 100 mM phosphate buffer pH 8, 5.0 mM 2, 4 dichlorophenol, 16.4 mM 4 – aminoantypyrene, 4 mM H_2O_2 and 100 µl culture supernatant. After addition of H_2O_2 the absorbance change at 510 nm was monitored for 5 min at 25°C and the activity was calculated by using molar absorptivity of 18,500 M^1 cm^1.

2.5.4. Polyphenol oxidase

The enzyme assay of polyphenol oxidase was carried out with spectrophotometrically by using 5mM L- DOPA as a substrate. The reaction mixture contains 2.80 ml buffer, 0.10 ml 5 mM L- DOPA, 0.10 ml 2.1mM Ascorbic acid and 0.10 ml enzyme solution against blank that is same reaction mixture accept enzyme and ascorbic acid. One unit activity will cause the change in A 265 $_{nm}$ of 0.001 per minute at pH 7 and at 25°C in 3 ml reaction mixture containing catechol and ascorbic acid [15].

2.5.5. Tyrosinase

The enzyme assay of tyrosinase was carried out with spectrophotometrically by using 1 mM L-Tyrosine solution as substrate. The reactions mixture contains 2.90 ml (reaction cocktail containing tyrosine and deionized water and buffer) and 0.10 ml enzyme solution against blank that is same reaction mixture accept enzyme. One unit activity will cause the change in A 280 $_{nm}$ of 0.001 per minute at pH 7 and at 25°C in 3 ml reaction mixture containing tyrosine [16].

2.6. Protein estimation

Protein estimation was done by the Lowry method using Bovine Serum Albumin as a standard [17].

2.7. Statistical analysis

Results obtained were the mean of three or more determinants. analysis of the variants was carried out on all data at $P< 0.05$ using Graph Pad software. (Graph Pad Instat version 3.00, Graph Pad software, San Diego, CA, USA)

3. RESULTS AND DISCUSSION

3.1. Growth of bacteria in lignin sulfonic acid sodium salt containing medium

Lignin structures complexity enables it to use as substrate to study mechanism of its degradation. These problems overcome by using common strategies includes use of lignin model compounds like in the degradation of Kraft indulin lignin [18] acetovanillone; vanillyl alcohol; guaiacol [19], and humic acid model compounds [20]. It was observed that the *Rhodococcus* NCIM 2891 was able to grow on lignin sulfonic acid sodium salt as a sole source of carbon. The maximum lignin sulfonic acid sodium salt degradation was observed by its structural changes observed in FTIR analysis after 10^{th} day from its inoculation point.

3.2. UV – visible spectrophotometer analysis

The degradation of lignin sulfonic acid sodium salt analyzed by UV – visible spectrophotometer it is observed that the control sample (control) gives absorption maxima from 200 to 305 where the test sample (broth with 10 and days incubation centrifuged sample) gives from 200 to 250 from here it decreases and second peak was observed at 280nm. **Figure-1**. The UV-visible characterization for the identification and determination of the concentration of acid soluble lignin by using hydrolysate according to [21].

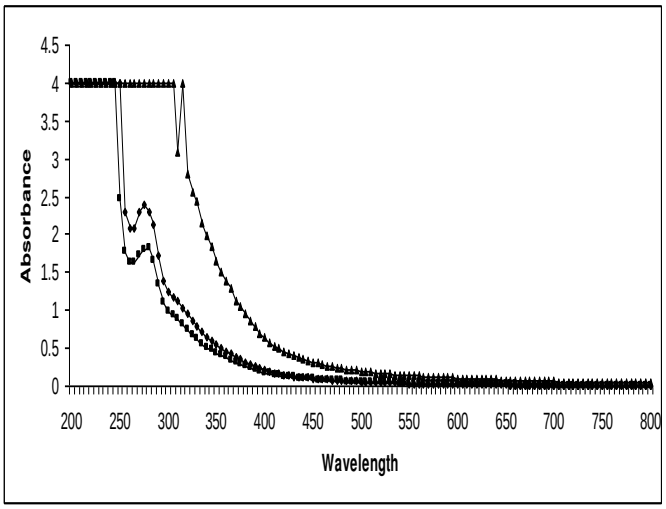

Figure-1. The UV/VB absorption maxima of control lignin sulfonic acid sodium salt (▲) and degraded product after 10 days (♦) and after 15 days (▪).

3.3. FTIR analysis

The observed peak at 860 Cm^{-1} and 1,068 Cm^{-1} which are originated from C–H out of plane and C– O in secondary alcohols, similarly the specific peak shifts for the degradation products of lignin sulfonic acid sodium salt were observed at 1,402 Cm^{-1} (S=O) for the sulfate residues, 1,364 Cm^{-1}(O-CH_2-O-) for esters of methylene scissors. 1,642 Cm^{-1} (C= O) for the quinones in 2 ring structure, 3,400 Cm^{-1} for (OH)

radicals and 2431 Cm^{-1} (–CHO) observed for aldehydes and denatured (R-OH) group. Where as in control sample the peaks were observed at 2,380 Cm^{-1}, 1,200 Cm^{-1}, 1,402 and at 1,190 Cm^{-1} that are in a range of known specific bands in FTIR analysis which are observed by [22] during their studies of degradation of lignin compound like Klason lignin and APPL samples under sulfate reducing condition. **Figure-2**. Fangeng and Zhuomin (2003) [23] obtained similar results during the electro degradation of lignosulfonates.

Figure-2. The FTIR analysis of control lignin sulfonic acid sodium salt (C) and degraded product (T).

3.4. GC-MS analysis

GC/MS, Py-GC/MS has several great advantages as a technique for enabling rapid analysis of partially biodegraded lignin and for yielding structural information that can contribute to a better understanding of the transformation of lignin macromolecules [24]. The obtained degraded compounds are compared with the standard structures that has been obtained by the NIST library the most probable structures with the respect to the enzymatic action on native compound are taken in to consideration and these compounds are analyzed The results obtained from extracted sample GC-MS reveals that the organism produces enzyme was capable to degrade lignin sulfonic acid sodium salt in its monomeric compounds viz toluene, propanaldehyde and 2-methyl benzaldehyde. The compounds were identified based on their retention time and the molecular weight obtained during analysis summarized in **Figure-3** [22] were obtained similar results by Py-GC/MS during their studies. These compounds are compared with the standard GC/MS peaks obtained from Japan AIST/NIMC Database [25]. From GC-MS data, it was observed

that the obtained compounds formed after degradation of lignin sulfonic acid sodium salt.

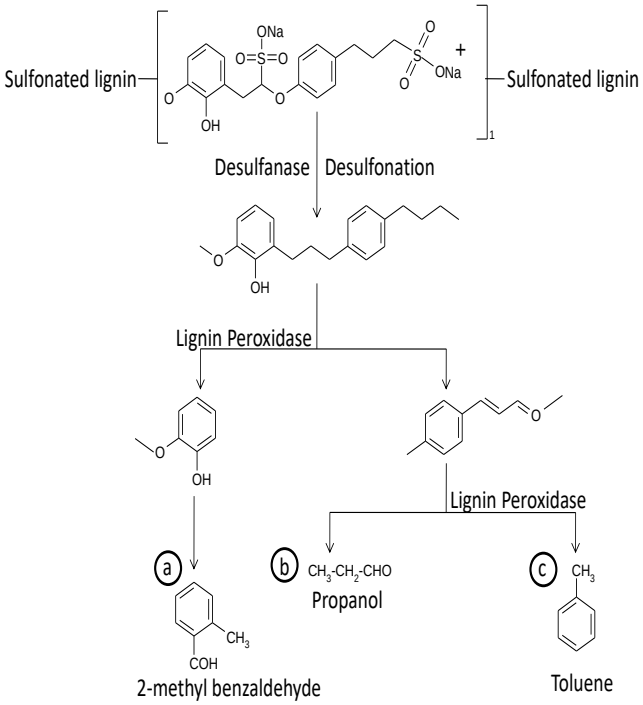

Figure-3. proposed pathway of lignin sulfonic acid sodium salt degradation by *Rhodococcus* NCIM 2891.

3.5. Purification of catechol 1, 2-dioxygenase

The purified catechol 1, 2-dioxygenase was obtained after 10 days of incubation in presence of lignin sulfonic acid sodium salt the purification profiles is given in **Figure-4** and the activity of purified catechol 1, 2-dioxygenases at different stages of purification were given in **Table-1**.

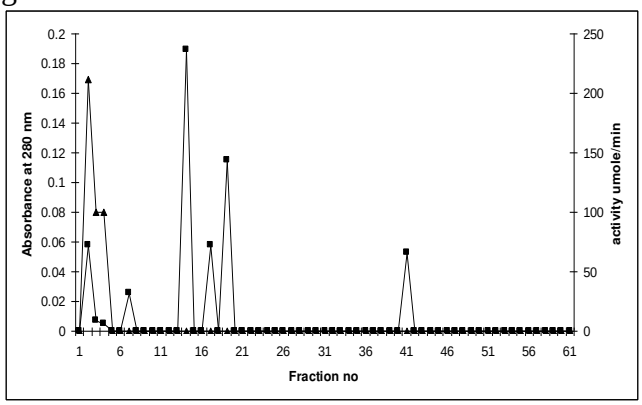

Figure-4. Elution profile of catechol 1, 2-dioxygenase from DEAE-cellulose column chromatography in presence of lignin sulphonic acid. Fractions from the DEAE-cellulose anion exchange chromatography (■) and fractions showing catechol 1, 2-dioxygenase activity (▲).

Table-1. Purification profile of enzymes polyphenol oxidase, Catechol 1, 2 dioxygenase.

Enzyme	**Enzyme activity(units)**	**Proteins(mg)**	**Sp activity (Units/mg of protein)**	**Yield %**	**Purification fold**
Catechol 1, 2 dioxygenase					
Enzyme	Enzyme activity(units)	Proteins(mg)	Sp activity (Units/mg of protein)	Yield %	Purification fold
Crude Extract	700	22.40 ± 0.03	31.25 ± 0.02	100	1
After ammonium sulfate precipitation	**a**				
After ion exchange chromatography	320	5 ± 0.02	64 ± 0.06	45.71	2.048

a - activity not determined.

The specific activity of catechol 1, 2-dioxygenase was measured about 65 µmole/mg of protein in lignin sulfonic acid sodium salt as a carbon source. SDS/PAGE analysis reveals that the enzyme has a molecular weight of 30kD as shown in **Figure-5**. There are reports of production of catechol 1, 2-dioxygenase from number of phenol and similar hydrocarbon degrading microorganisms like *Ralstonia* sp, *Pseudomonas aeruginosa, Rhodococcus sp*. AN-22, *R. rhodochrous* NCIMB 13259 strains [26-28]. with phenol as substrate. The SDS/PAGE analysis shows that the molecular weight of the catechol 1, 2-dioxygenase from *Rhodococcus* NCIM 2891 was near about 30 KD which was similar to that of *Ralstonia* sp. Ba-0323 (30 KD) [27].

The difference was that the *Ralstonia spp* has not been reported to grow in presence of lignin sulfonic acid sodium salt whereas *Rhodococcus* NCIM 2891 could grow in presence of lignin sulphonic acid sodium salt at a concentration of 1gm L^{-1} and produce this enzyme.

From obtained results it was seen that the catechol 1, 2 dioxygenase was the key enzyme that has been produced by different types of microorganisms with response

to different type of substrates but there was no reports of the catechol 1,2 dioxygenase production during the lignin degradation as it bears the potential to convert simple lignin degraded products in to TCA cycle intermediates and it can be working as an key intermediate enzyme in complete mineralization of complex substance like lignin sulfonic acid sodium salt.

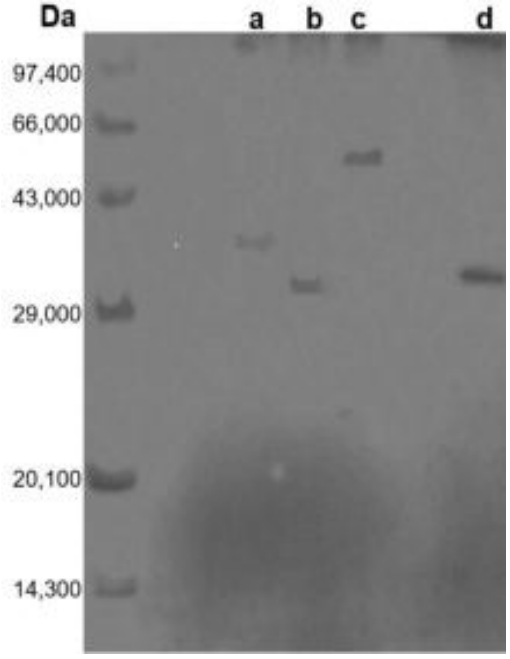

Figure-5. SDS-PAGE of purified Tyrosinase (a) catechol oxidase (b), polyphenol oxidase(c) and catechol 1, 2-dioxygenase (d).

3.6. Purification of extracellular phenol oxidases and lignin peroxidase

Polyphenol oxidases like catechol oxidases, tyrosinase, polyphenol oxidases are an unusual monooxygenase in that it does not require a reducing cofactor such as NADH [29]. The enzyme activities at different Stages of purification and purification profile of DEAE - Cellulose ion exchange column chromatography of catechol oxidase, polyphenol oxidase and tyrosinase in medium containing lignin sulfonic acid sodium salt are given in **Table-2** and **Figure-6**.

Table-2. Purification profile of enzymes polyphenol oxidase, Catechol oxidase, Tyrosinase and Lignin peroxidase.

Enzyme	Enzyme activity(units)	Proteins(mg)	Sp activity (Units/mg of protein)	Yield %	Purification fold
Polyphenol oxidase					
Crude	54	130 ± 0.09	0.4 ± 0.05	100	1
After ammonium sulfate precipitation	39	14 ± 0.05	2.7 ± 0.06	72.22	6.75
After ion exchange chromatography	22	0.700 ± 0.05	31.42 ± 0.05	40.74	78.55
Catechol oxidase					
Crude	65	130 ± 0.09	0.5 ± 0.08	100	1
After ammonium sulfate precipitation	57	14 ± 0.05	4.07 ± 0.07	87.69	8.14
After ion exchange chromatography	26	0.800 ± 0.04	32.5 ± 0.06	40	65
Tyrosinase					
Crude	a				
After ammonium sulfate precipitation	140	14 ± 0.05	10 ± 0.03	100	1
After ion exchange chromatography	170	9 ± 0.03	18.8 ± 0.06	121.4	1.88
Lignin peroxidase					
Crude	129	130 ± 0.09	0.9 0.04	100	1
After ammonium sulfate precipitation	118	14 ± 0.05	8.4 ± 0.06	91.47	9.33
After ion exchange chromatography	a				

a - activity not determined.

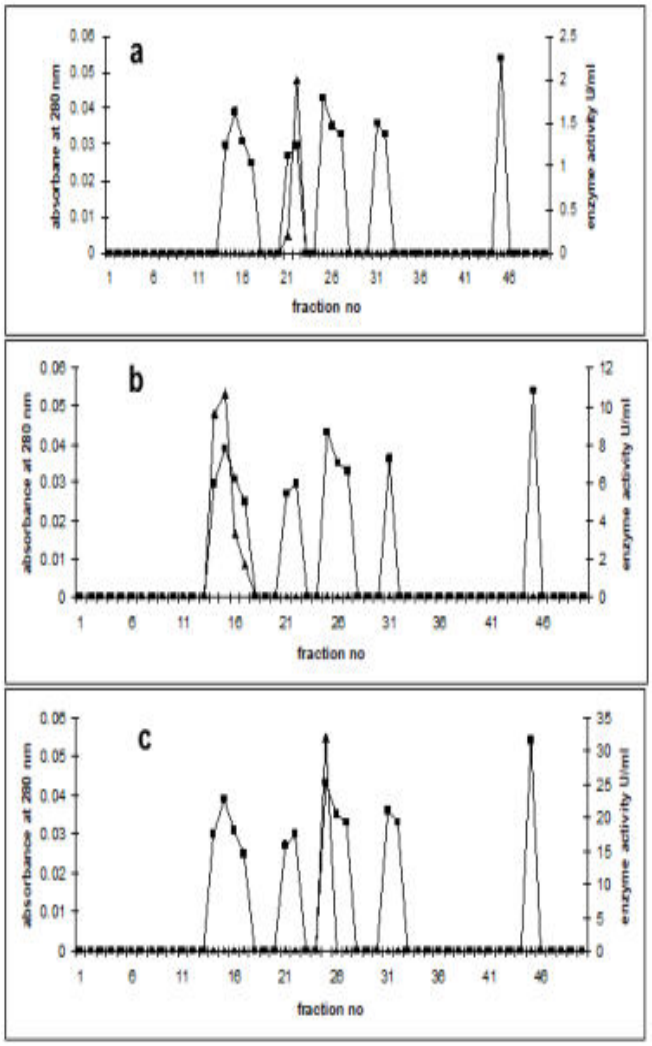

Figure-6. The elution profile of and polyphenol oxidase (a) catechol oxidase (b) tyrosinase (c) Fractions from the DEAE-cellulose anion exchange chromatography (■) and fractions showing enzyme activity (▲).

A wide variety of o-dihydroxy phenols, such a caffeic acid derivatives, can also act as good substrates for polyphenol oxidases. Polyphenol oxidase oxidation of monophenols and o-diphenols has been studied extensively, even though some of these substrates are not natural compounds. [30]. From **Table-2** the enzyme activities obtained from lignin sulfonic acid sodium salt are as follows polyphenol oxidase (31.42U/mg of protein); catechol oxidase (32.5U/mg of protein); tyrosinase (18.8U/mg of protein) and Lignin peroxidase (8.4U/mg of protein). SDS/PAGE analysis reveals that these enzymes have molecular weight as follows tyrosinase 36kDa. The molecular weight of tyrosinaseranges from 18 kDa to 75 kDa. The

molecular weight of *Rhodococcus* tyrosinase are similar with the tyrosinase of *Vibrio tyrosinaticus* [31]. The molecular weight of polyphenol oxidase was measures 50kDa which is more than the polyphenol oxidase of *Neurospora crassa,* has a molecular weight of 46,000 Da [32]. The molecular weight of catechol oxidase was seen to be 30 kDa whereas the molecular weights calculated for bacteria are in a range of 28kDa to 32kDa [33]. The SDS/PAGE analyses of enzymes are shown in **Figure-5.**

4. CONCLUSION

Various chemical and physical methods are used for removing both inorganic and organic sulfur containing compounds and degradation of these compounds including lignites and other sulfur compounds like lignosulfonates, that are generated in industrial processing are time consuming and costly. The advantages of the microbial process over these conventional methods are not only energy effective but are also cost effective. The present study gives the most optimum results for the extracellular polyphenol oxidases, peroxidase like enzyme lignin peroxidase and catechol 1, 2-dioxygenase in presence of lignin sulfonic acid sodium salt as a sole source of carbon. However, all known microorganism involved in lignin degradation will not have the same capacity of degradation and expression of enzymes for degradation for sulfonated polymers like lignosulfonates. In conclusion lignin sulfonic acid sodium salt will be a best alternative substrate for the detection and studies related to degradation of lignin like polymers and enzymes involved in their degradation by microorganisms bearing desulfurization and desulfonation activity like *Rhodococcus* NCIM 2891. It was also observed that the lignin sulfonic acid sodium salt (Mol Wt. 50,000 Da) is preliminary cleaved by the peroxidases than the other oxidases formed during the incubation period. It is evident that lignin molecule denatured by lignin peroxidase and other phenol oxidases into their simple and utilizable form like catechols or quinones can be further degraded by cells with ring cleaving enzymes like catechol oxidases in to metabolic intermediates. These findings of *Rhodococcus* NCIM 2891 can be utilized to optimize biodegradation and bioremediation of many phenolics like lignin sulfonic acid in the environment to protect the natural biodiversity of the system.

ACKNOWLEDGEMENTS

Authors are thankful to Department of Microbiology, Shivaji University, Kolhapur, to extending their lab facilities for fulfillment of these work.

REFERENCES

1. Nandan, R., Raisuddin, S. In Fungal degradation of industrial wastes and waste water, edited by Murkerji, K. G. Health and Environmental Research Online, (1992) pp.931–61.
2. Martin, V. J., Yu, Z., Mhon, W. W. (1999) Archives of Microbiology, 172, 131–138.
3. Hammel, K. E. In Metal ions in biological systems, edited by Sigel, H., Sigel, A. Marcel Dekker, (1992) pp.41-60.
4. Field, J. A., Jong, E., Feijoo-Costa, G., Bont J. A. M. (1993) Trends in Biotechnology, 11, 44–49.
5. Paszczynski, A., Crawford R. L. (1995) Biotechnology Progress, 11, 368–79.
6. Crawford, R. L. (1981) American Birds, 35, 913-914.
7. Hatakka, A. (1994) FEMS Microbiology Reviews, 13, 125–35.
8. Loh, K. C., Tan, C. P. P. (2000) Bulletin of Environmental Contamination Toxicology, 64, 756–63.
9. Funazukuri, T., Cho, J. S., Wakao, N. (1980) Fuel, 69, 1328–1329.
10. Naae, D. G., Whittington, L. E., Ledoux, W. A., Debons, F. E. (1988) Surfactants from Lignin, 4, 739-040.
11. Yang, W., Jianping, J., Xiaoqiang, C., Qinggele., Zongding, H. (2006) American Society for Microbiology, 73, 226–231.
12. Bell, K. S., Philp, J. C., Aw, D. W. J., Christofi, N. (1998) Journal of Applied Microbiology, 85, 195–210.
13. Laemmli, U. K. (1970) Nature, 227, 682-685.
14. Aoki, K., Konohana, T., Shinke, R., Nishira H. (1984) Agricultural Biological Chemistry, 48, 2087–2095.
15. Marumo, K., Waite, J. H. (1986) Biochemistry Biophysics Acta, 872, 98-103.
16. Duckworth, H. W., Coleman, J. E. (1970) Journal of Biological Chemistry, 245, 1613-1625.
17. Lowry, O. H., Rosebrough, N. J., Farr, A. L., and Randall, R. J. (1951) Journal of Biological Chemistry, 193, 265-275.
18. Giroux, H., Vidal, P., Bouchard, J., Lamy, F. (1988) Applied Environmental Microbiology, 54, 3064- 3070.
19. Spiker, J. K., Crawford, D. L., Thiel, E. C. (1992) Applied Microbiology Biotechnology, 37, 518-523.
20. Kontchou, C. Y., Blondeau, R. (1991) Canadian Journal of Microbiology, 38, 203-208.
21. Dence, C.W. In Methods in Lignin Chemistry, edited by Lin, S. Y., Dence, C.W. Springer, (1992) pp.33–61.

22. Jae-Jung, K., Yoshihisa, S., Kazuhiro, I., Seog-Ku, K., Chul-Hwi, P., Saburo, M. (2009) Bioresource Technology, 100, 1622–1627.
23. Fangeng, C., Zhuomin, L., Bin, T. (2003) Journal of Wood Chemistry and Technology, 23, 261–277.
24. Telysheva, G., Dobele, G., Meier, D., Dizhbite, T., Rossinska, G., Jurkjane, V. (2007) Journal of Analytical and Applied Pyrolysis, 79, 52–60.
25. http://webbook.nist.gov/chemistry.
26. Strachan, P. D., Freer, A. A., Fewson, C. A. (1998) Journal of Biochemistry, 333, 741–747.
27. Wang, C. L., Takenaka, S., Murakami, S., Aoki, K. (2001) Bioscience Biotechnology Biochemistry, 65, 1957–647.
28. Chuan, L. W., Su, L. Y., and San, L. W. (2006) Process Biochemistry, 41, 1594 –160.
29. Aitken, M. D. (1993) Journal of Chemical Engineering, 52, 49–58.
30. Jime´nez, M., Garcı´a Carmona, F. (1999) Journal of Agriculture and Food Chemistry, 47, 56–60.
31. Harold, C., Heinz, D. (2006) Systematic and Applied Microbiology, 29, 3–14.
32. Whitaker, J. R. In Principles of Enzymology for the Food Sciences, edited by Whitaker, J. R. Elsevier, (1994) pp.49.
33. William H., F., Jennifer K. I. (2008) Journal of Inorganic Biochemistry, 102, 2160–2170.

Green Synthesis of Zinc Oxide Nanoparticles from Heena (*Lawsonia inermis*) Leaves Extract and its Antibacterial Potential

Pranoti N. Kirdat[a], Prerana P. Shevate [b], Sanchita S. Dekhane[b], Kshitija D. Chavan[b], Bhakti D. Jadhav[b], Padma B. Dandge[a,*]

[a]Department of Biochemistry, Shivaji University, Kolhapur 416 004 (MS) India.
[b]Department of Nanoscience and Technology, Y.C.I.S.Satara 415 002 (MS) India.
[*]Corresponding author: pbd_biochem@unishivaji.ac.in

ABSTRACT

Biological method of nanoparticles synthesis is simple, easy, eco-friendly, and cost effective. The zinc oxide nanoparticles are mainly synthesized by chemical method, but now-a-days biological method is preferable. In current study zinc oxide nanoparticles synthesized by using heena (Lawsonia inermis) leaves extract which acts as a reducing agent and zinc nitrate as a precursor. The zinc oxide nanoparticles were confirmed by UV- visible spectroscopy, Fourier transform infrared spectroscopy (FTIR), X- ray diffraction technique (XRD) and Scanning electron microscopy (SEM). The Zinc oxide nanoparticles showed characteristic peak at 343 nm. The different functional groups attached to it were analyzed by FTIR spectroscopy. In X-ray diffraction analysis, it showed highest peak at (101) crystal plane with 2 θ value 37.37. The surface morphology analyzed by SEM which showed stabilized and irregular rhombus like structure of zinc oxide nanoparticles. The biologically synthesized zinc oxide nanoparticles from Lawsonia inermis exhibited antibacterial activity against Gram positive B.subtilis and Gram negative E.coli bacteria with zone of inhibition of 17 mm and 19 mm diameter. This new approach for synthesis of zinc oxide nanoparticles is more appropriate for the efficient synthesis of nanoparticles.

KEYWORDS

Lawsonia inermis, Zinc nitrate, Zinc oxide nanoparticles, Antibacterial activity.

……

1. INTRODUCTION

Nanotechnology is interdisciplinary field of research which connects material science, bio-nanoscience and technology. The specific morphological properties of nanoparticles have crucial importance in nanoscience studies. Nanoscience controls size of particles and generates new material with property within range 1-100 nm.

Thus; it extends vast area of research in today's scenario. At the nano level, particles show totally new characteristics related to size and morphology. Recent development in the field of nanoscience and nanotechnology helps to improve different areas of research. Potential applications of these nanostructures have observed in various fields like catalysis, sensors, water purification, nanomedicines and nanoelectronics [1, 2].

The conventional physico-chemical methods of synthesizing nanoparticle were more expensive, require increased time and utilize hazardous chemicals which may cause environmental pollution. To minimize the use of harmful chemicals, researchers try to develop a green synthesis perspective for the synthesis of nanoparticles [3]. Thus, environmentally friendly, cost-effective biological method for synthesis of nanoparticles was developed. The biological things such as microorganisms, fungi and plant extract were used, so it also called biogenic synthesis of nanoparticles. Out of these biological things, plant extract is commonly used because of its easy availability and simple procedure. The secondary metabolites present in plant extract acts as capping agent which help to reduce precursor of particle into its nano form. Due to low toxicity the nanoparticles synthesized using the plant system can be utilized for different commercial applications like pharmaceuticals, food packaging, nanomedicine, etc. [4].

In recent era, zinc oxide nanoparticles (ZnO NP) were studied by many researchers due to its distinctive optical and chemical behavior, unique antibacterial, antifungal, UV filtering properties, high catalytic and photochemical activity. Among all metal oxide nanoparticles, zinc oxide nanoparticles have tremendous applications in electronics, cosmetics, pharmaceutical, communication, sensor and environmental protection. Zinc Oxide nanoparticles has potential applications in biomedical field like biological sensing, gene delivery, drug delivery and nanomedicine also it has antifungal and antioxidant ability as well as antimicrobial activity against Gram positive and Gram negative micro-organisms. ZnO nanoparticles were less toxic and safer than other nanoparticles so they have remarkable applications in food, cosmetic industry, solar cells and semiconductors [5,6,7].

Lawsonia inermis (Mehendi) is commercially known as heena leaves. It is a small shrub with different medicinal values. The phytochemical secondary metabolites like tannins, terpenoids, flavonoids that have been demonstrated to have antibacterial potential and acts as reducing agent during the synthesis of zinc oxide nanoparticles [8]. Its stem bark, roots, flowers and seeds have also been used in conventional medicines. It has been traditionally reported in use of headache, bleeding disorder, skin diseases, antibacterial, antifungal, antioxidant and anti-dandruff agent. Thus, present study is based on simple and rapid synthesis and

characterization of zinc oxide nanoparticles from leaves extract of heena for its antibacterial applications.

2. EXPERIMENTAL SECTION

2.1. Preparation of leaves extract

Fresh leaves of heena were collected from botanical garden Y.C.I.S.Satara, Maharashtra, India. These leaves were thoroughly washed and cut into fine pieces.15 gram of leaves were added into 150 ml D/W and stirred for 1 hour at 30°C-40°C. The filtrate was collected and used for further synthesis process.

2.2. Preparation of precursor

For the synthesis of nanoparticles zinc nitrate was used as precursor.0.1M zinc nitrate was prepared into100 ml D/W and stored it.

2.3. Synthesis of nanoparticles

Fresh extract of heena leaves extract and zinc nitrate precursor was taken in 1:2 ratio. 20 ml of leaves extract was kept for stirring and drop wise addition of 40 ml zinc nitrate was done. The resulting mixture was stirred for 1 hr at 30°C-40°C which gives wine red color and precipitate was settled at bottom. The precipitate was collected by filtration, washed D/W and ethanol to remove any impurities. The precipitate contains white colored zinc oxide nanoparticles. It was kept for air drying for 24 hr and annealed in muffle furnace. The resulting white colored powder was used for characterization and applicatory studies.

2.4. Antibacterial assay

The antibacterial activity of synthesized ZnO nanoparticles was studied against Gram positive *Bacillus subtilis* and Gram-negative *Escherichia coli* obtained from Department of Biochemistry, Shivaji University, Kolhapur. The nutrient agar plates were prepared and 0.1 ml of *B.subtilis* and *E.coli* suspension was spread on plate with sterilized spreader. Wells were bored in each plate by using sterilized borer. Add different concentrations of henna leaves extract and synthesized nanoparticles into each well. Plates were kept into incubator for 24 hr at 37°C and observed for zone of inhibition on next day.

3. RESULT AND DISCUSSION

3.1. UV-visible spectroscopy

The color change is the key point which confirms formation of nanoparticles in solution and analyzed by UV-visible spectroscopy. It gives primary characterization of nanoparticles. The UV absorption spectra of nanoparticles were affected by some parameters like method of synthesis, temperature as well as size and shape of nanoparticles [9]. The UV-visible spectra of synthesized zinc oxide nanoparticles

were recorded at room temperature between 200-600 nm against D/W as a reference. Due to surface plasmon resonance, ZnO nanoparticles exhibited characteristics peak at 343 nm with band gap 3.61 eV (**Figure-1**).

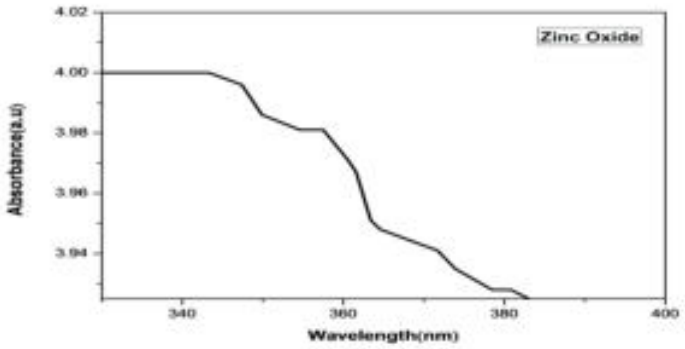

Figure-1. UV-visible spectrum of ZnO nanoparticles.

3.2. Fourier transforms infrared (FT-IR) spectroscopy

The FT-IR spectra of synthesized ZnO nanoparticles were recorded between 500-4000 cm^{-1} (**Figure-2**). The different functional groups attached to nanoparticles were analyzed by this spectroscopy. The peak at 3438.46 cm^{-1}corresponds to O-H bond stretching [10]. The peak at 2929.34 cm^{-1} and 2859.92 cm^{-1} corresponds to C-H stretching which indicates strong capping on zinc oxide nanoparticles [11]. Primary amines were present at 1637.27 cm^{-1} [12]. Zn-O vibrational stretching was given by 458.98 cm^{-1}[13].

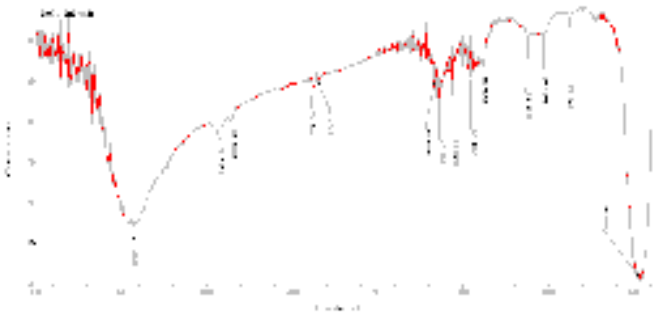

Figure-2. FTIR analysis of ZnO nanoparticles.

3.3. X-ray Diffraction (XRD)

X-ray diffraction analysis of synthesized ZnO nanoparticles was carried out to determine size of nanoparticles by Debye-Scherrer equation. Size of nanoparticles was calculated from highest peak (figure-3). The 2θ values determined from XRD graph are 32.82, 32.94 and 35.35 with (hkl) planes (100, 002 and 101) respectively.

The size of synthesized ZnO nanoparticles was found to be 4.71nm (47A^{o}) with 2θ value 35.35 and (hkl) plane is (101). (JCPDS card no. 76-0704) [14, 15, 16].

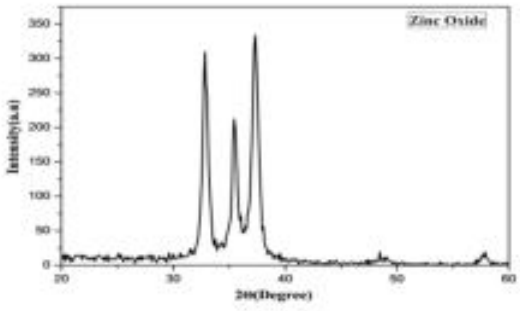

Figure-3. XRD analysis of ZnO nanoparticles.

3.4. Scanning electron microscopy (SEM)

Scanning electron microscopy is used to study surface morphology of nanoparticles. Agglomerations of nanoparticles were observed in SEM analysis [17]. The synthesized ZnO nanoparticles showed stabilized irregular rhombus like structure in SEM analysis (**Figure-4**).

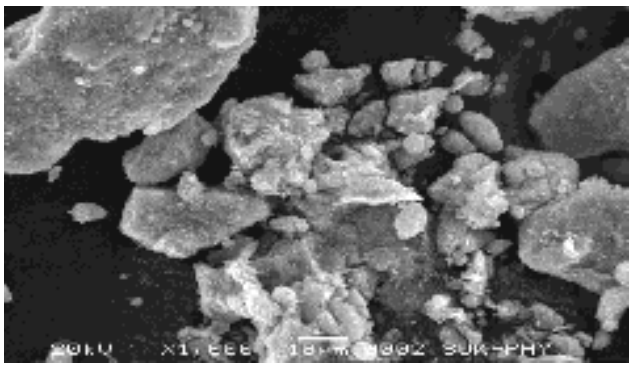

Figure-4. SEM analysis of ZnO nanoparticles.

3.5. Antibacterial activity

The activity was studied by using agar well diffusion method. The antibacterial activity of heena leaves extract and synthesized zinc oxide nanoparticles was studied against Gram positive *B.subtilis* and Gram negative *E.coli* bacteria. The extract contains different phytochemicals and secondary metabolites which acts as antibacterial agent and also impart antibacterial potential to synthesized ZnO nanoparticles. Antibacterial activity of nanoparticles depends on the particle size, stability, concentration of nanoparticles, concentration of growth medium and type of bacteria tested against nanoparticles.

In the present study, microbial pathogen Gram positive *Bacillus subtilis* and Gram-negative *Escherichia coli* were used. After incubation of 24 hr the petri plates were observed for zone of inhibition. The different concentrations from 20 µl to 120 µl of heena leaves extract and ZnO nanoparticles were used. The maximum inhibition zone was observed at 120 µl for both micro-organisms ZnO nanoparticles showed 19 mm and 17 mm inhibition zone for *E.coli* and *B.subtilis* respectively (**Figure-5** and **Figure-6**). From the zone of inhibition, it was concluded that ZnO nanoparticles showed good antibacterial activity against Gram negative micro-organisms than heena leaves extract.

The following observation table (**Table-1**) depicted zone of inhibition by heena leaves extract and zinc oxide nanoparticles against *E.coli* and *B. subtilis*:-

Table-1. Zone of inhibition by leaves extract and ZnO nanoparticles.

Sr.no.	**Bacteria**	**Concentration (µl)**	**Zone of inhibition (mm)**	
			Heena leaves extract	**Zinc oxide nanoparticles**
1.	*E.coli*	20	-	-
		40	-	-
		60	-	-
		80	-	12
		100	-	14
		120	-	19
2.	*B.subtilis*	20	-	-
		40	-	-
		60	-	-
		80	-	11
		100	-	13
		120	-	17

Figure-5. Zone of inhibition by ZnO nanoparticles against *E.coli.*

Figure-6. Zone of inhibition by ZnO nanoparticles against *B. subtilis.*

4. CONCLUSION

Biological synthesis of zinc oxide nanoparticles using leaves extract of heena (*Lawsonia inermis*) was carried of successfully. The synthesized nanoparticles were studied for their optical and structural properties by using UV- visible spectroscopy, FTIR spectroscopy, X-ray diffraction technique and SEM analysis. In UV-visible spectrum, it showed characteristic absorption peak at 343 nm. The FTIR analysis showed presence of different functional groups. The size of nanoparticles is 4.71 nm analyzed from XRD. The stabilized irregular rhombus like structure was observed in SEM analysis. The antibacterial activity of zinc oxide nanoparticles was studied against Gram positive and negative bacteria showed that zinc oxide nanoparticles were potential antibacterial agent for Gram negative *Escherichia coli*. Thus, due to eco-friendly, rapid and easy synthesis method, small size and good antibacterial activity zinc oxide nanoparticles can be used for various environmental and biomedical applications.

ACKNOWLEDGMENT

The authors are thankful to Department of Nanoscience and Technology, Y.C.I.S.Satara and Department of Biochemistry, Shivaji University, Kolhapur for providing all research facilities to carry out this work.

REFERENCES

1. Ratney, Y. J. J., David, S. B. In International Journal of Latest Trends in Engineering and Technology, edited by Jeba Jane Ratney, Y. J. Oxford, (2017) pp.010-015.

2. Varghese, E., George, M. (2015) International Journal of Advance Research
in Science, Engineering and Technology, 4, 307- 314.
3. Kirdat, P. N., Dandge, P. B., Hagwane, R. M., Nikam, A. S., Mahadik, S. P. Jirange, S. T. (2021) Materials Today, 43, 2826-2831.
4. Lakshmi, S. J., Roopa Bai, R. S., Sharanagouda, H., Ramachandra, C. T., Nidoni, U. K. (2018) Journal of Pharmacognosy and Phytochemistry, 7, 10-14.
5. Kalpana, V. N., Chakraborthi, P., Devi, R. V. (2018) Bioinorganic Chemistry
and Applications, 1-12.
6. Parthasarathy, G., Saroja M., Venkatachalam, M., Evanjelene, V. K. (2017) International Journal of Materials Science, 12, 73-86.
7. Santhoshkumar, J., Venkat, K. S. Rajeshkumar, S. (2017) Biochemistry and Biophysics reports, 11, 46-57.
8. Upadhyaya, H., Shome, S., Sarma, R., Tewari, S., Bhattacharya, M. K., Panda, S. K. (2018) American Journal of Plant Sciences, 9, 1279-1291.
9. Safawoa, T., Sandeepa, B. B., Polaa, S. Tadesse, A. (2018) Open Nano, 56–63.
10. Srivastava, V., Gusain D., Sharma Y. C. (2013) Ceramics International, 39, 9803–9808.
11. Chaudhuri, S. K., Malodia, L. (2017) Applied Nanoscience, 7, 501–512.
12. Datta, A., Patra, C., Bharadwaj, H., Kaur, S., Dimri, N., Khajuria, R. (2017) Journal of Biotechnology and Biomaterials, 7, 271-276.
13. Rajendran, S. P., Sengodan, K. (2017) Journal of Nanoscience, 2017.
14. Umar, H., Kavaz D., Rizaner N. (2019) International Journal of Nanomedicine, 14, 87.
15. Ogunyemi, S. O., Abdallah Y., Zhang M., Fouad H., Hong X., Ibrahim E., Masum M. I., Hossain A., Mo, J., Li, B. (2019) Artificial Cells, Nanomedicine and Biotechnology, 47, 341-352.
16. Geetha, A., Sakthivel, R., Mallika, J., Kannusamy, R., Rajendran, R. (2016)
Oriental journal of chemistry, 32, 955-963.
17. Suresh, J., Pradheesh, G., Alexramani, V., Sundrarajan, M., Hong, S. I. (2018) Advances in Natural Sciences: Nanoscience and Nanotechnology, 9,
015008.

Antibacterial Activity of Nickel Oxide nanoparticles Synthesized from Tulsi (*Ocimumtenuiflorum*) Leaves Extract

Pranoti N. Kirdat[a], Sandip S. Kale[a], Salma H. Nadaf[a], Sneha N. Lawand[b], Sharvari P.Takale[b], Padma B. Dandge[a,*]

[a]Department of Biochemistry, Shivaji University, Kolhapur 416 004 (MS) India.
[b]Department of Nanoscience and Technology, Y.C.I.S. Satara 415 002 (MS) India.
[*]Corresponding author: pbd_biochem@unishivaji.ac.in

ABSTRACT

Synthesis of nickel oxide nanoparticles using biological entities is cost effective and eco-friendly approach. In current study, nickel oxide nanoparticles (NiO) synthesized by utilizing tulsi (Ocimum tenuiflorum) leaves extract which reduces nickel chloride precursor into its nano form. The structural properties of nanoparticles were confirmed by UV- visible spectroscopy, Fourier transform infrared spectroscopy (FTIR) and X- ray diffraction technique (XRD). The NiO nanoparticles exhibited characteristic peak at 379 nm with band gap 3.27 eV while FTIR spectroscopy analyzes different functional groups attached to it. In X-ray diffraction analysis NiO nanoparticles revealed sharp and highest peak at (220) with 2 ɵ value 52.59 and also exhibited single crystalline structure having tetragonal cubic phase with 3.37 nm size. The biologically synthesized nickel oxide nanoparticles from Ocimum tenuiflorum leaves extract showed antibacterial activity against Gram positive Staphylococcus aureus and Gram negative Escherichia coli.Thus,NiO nanoparticles can be utilized as potential antibacterial agent against range of micro-organisms.The synthesis of NiO nanoparticles using leaves extract is more appropriate strategy for the effective synthesis of nanoparticles.

KEYWORDS

Ocimum tenuiflorum, Nickel oxide nanoparticles, Staphylococcus aureus, Escherichia coli, Antibacterial agent.

…….

1. INTRODUCTION

Nanoscience and Nanotechnology is the innovative branch of science that deals with production of nanoparticles with improved properties which are contrast from subsequent solid-state material and its applications. The size and properties

alterations are due to quantum size, surface to volume ratio and macroscopic tunnelling effect. The various physical and chemical techniques were employed for synthesis of metal oxide nanoparticles. But these methods are costly, time consuming and may cause some environmental effects due to utilization of harmful chemicals. Therefore, biological method for nanoparticles synthesis was developed to minimize impacts of harmful chemicals. Synthesis of nanoparticles using biological entities iseco-friendly, cost effective, minimum use of chemicals and requires less time for synthesis [1].

Amongst the all metals, magnetic transition metal dependent nanoparticles of Nickel, Copper and Iron was synthesized due to its superior magnetic properties and various applications. The crucial feature of Nanobiotechnology is the combination of biological principles with physical and chemical approach so as to synthesize nano sized particles with distinctive functions. Several procedures are performed to control the size and shape of nanoparticles [2]. The various biological things were employed for synthesis of nanoparticles but utilization of plant extracts specifically leaves showed significant formation of nanoparticles. The several secondary metabolites like terpenoids, flavonoids, phenols and alkaloids were present in leaves extract. These metabolites act as reducing agent which reduces bulk precursor into its nanoparticle form. The solvents with varying degree of polarity also effects on the synthesis of metallic nanoparticles [3]. There are certain basic requirements in biological synthesis; it includes i) choice of proper solvent, ii) an eco-friendly reducing agent and iii) non-toxic stabilizing agent for nanoparticles. Therefore, by maintaining suitable conditions biological method produces nanoparticles with controlled morphology without generation of harmful by-products. The materials synthesized by eco-friendly approach possess wide applications in biomedical and pharmaceutical industries [4]. The advantages behind the utilization of plant extract mediated metal nanoparticle synthesis is that, they are easily available, safe, non-toxic and contain large variety of phytochemicals which acts as effective reducing and capping agent. Thus, due to these benefits plant extracts easily converts bulk precursor into its nano form than microbial and fungi mediated nanoparticles synthesis [5].

Ocimum tenuiflorum, a small medicinal herb belongs to the family Lamiaceae commonly known as Holy Basil or Tulsi. The phytochemical constituents of tulsi consist of oleanolic acid, ursolic aid, rosmarinic acid, eugenol etc. while the essential oils are β-elemene, β-caryophyllene and germacrene. There are two nano forms of nickel that are nickel metal and nickel oxide. These two classes exhibited specific properties like magnetic, biocompatibility, catalytic activity, antimicrobial potential and sorption nature. Also, this nano sized nickel oxide nanoparticles (NiO) with band gap 3.6-4.9 eV behaves as semiconductor with high chemical stability and electron transfer efficiency. Hence, these NiO nanoparticles have wide applications in diverse

fields like electronics, energy devices, nanomedicines, sensors, waste water treatment and in the various organic synthesis such as reduction, hydrogenation, alkylation etc. [6]. In recent decades, plant extracts, micro-organisms, fungi and some enzymes were exploited for the synthesis of NiO nanoparticles. Thus, it results in development of green protocol approach.Among, all the biological things, plant extract attracts more attention because it acts as an effective capping agent and also helps to control size morphology of nanoparticles to prevent its agglomeration [7].

In current study, the synthesis of nickel oxide nanoparticles using *Ocimum tenuiflorum* leaves extract was carried out by using nickel chloride as precursor while ethanol and water used as solvent. The synthesized nanoparticles were characterized by UV-visible spectroscopy; Fourier transform infrared spectroscopy (FTIR) and X-ray diffraction (XRD). The antibacterial activity of prepared nanoparticles were studied against Gram positive and Gram negative micro-organisms.

2. EXPERIMENTAL METHODOLOGY

2.1. Preparation of Ocimum tenuiflorum leaves extract and precursor

Fresh leaves of *Ocimum tenuiflorum (tulsi)* were collected from botanical garden of Y.C.I.S. Satara, Maharashtra India. The leaves were washed with distilled water (D/W) to remove debris on it. These leaves were cut into fine pieces and crushed with minimum amount of D/W. 25 gm of crushed leaves were stirred along with 100ml of D/W and ethanol in 1:1 proportion at 80ºC for 2 hr. After stirring, resultant mixture was filtered through Whatmann filter paper and filtrate was used for synthesis of NiO nanoparticles. Pure 0.1mM nickel chloride (HiMedia,India) was dissolved in 100 ml of D/W and utilized as precursor for nanoparticle synthesis.

2.2. Synthesis of Nickel Oxide nanoparticles

The prepared leaves extract was mixed with 0.1 mM nickel chloride in 1:3 proportions with drop wise addition and stirring at 80^{o}C for 3 hr on magnetic stirrer. The resulting solution was annealed in furnace at 200°C for 2 hr. After annealing, black brown colored powder was obtained. Further, it was washed with ethanol to remove any other impurities. The purified powder was employed for further characterization and antibacterial studies.

2.3. Antibacterial activity

The bacterial strains were collected from Department of Biochemistry, SUK. The antibacterial activity of synthesized NiO nanoparticles was studied against Gram positive *Staphylococcus aureus* and Gram-negative *Escherichia coli* by using agar well diffusion method. The nutrient agar plates were prepared by traditional method and 100µl of *S.aureus* and *E.coli* suspension was spread on plate with sterilized spreader. Well, were prepared on each plate with the help of a sterilized borer. Add 50 µland 100 µl of synthesized nanoparticles into 2 wells while 50 µl of leaves

extract in another well as control. Plates were kept for incubation at 37°C for 24 hr. Zone of inhibition was observed on next day to determine the antibacterial activity. The zone was measured to determine the effectiveness of nickel oxide nanoparticles against these pathogens.

3. RESULT AND DISCUSSION

3.1. UV-Visible spectroscopy

The colour variation in solution is determined by UV–visible spectroscopy which is the basic characterization technique to study nanoparticles. The UV–visible spectra of synthesized NiO nanoparticles were noted at room temperature between 200 and 800 nm against D/W as a reference. The **Figure-1** indicates the UV-Visible spectrum of synthesized NiO nanoparticles from *tulsi* leaves extract. Due to surface plasmon resonance, NiO nanoparticles exhibited characteristics peak at 379 nm with band gap (Eg) 3.27 eV. The UV absorption also depends on size and shape of nanoparticles [8].

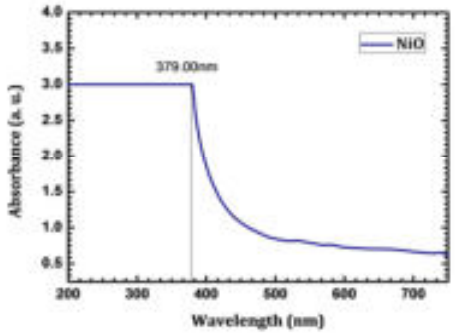

Figure-1. UV Visible spectrum of NiO nanoparticles.

3.2. Fourier transforms infrared spectroscopy (FTIR)

The FTIR spectroscopyanalysis of synthesized NiO nanoparticles was carried out between 500 and 4000 cm-1. The different functional groups attached to NiO nanoparticles surface were analysed by FTIR spectroscopy. The **Figure-2** represents the FTIR spectrum of prepared NiO nanoparticles. The small peak at 580.28 cm-1 corresponds to metal-oxygen stretching frequencies are related to Ni-O [8]. The small absorption band at 2920.68 cm-1 is due to the extending vibration mode of CO2, which occurred due to presence of aerial CO2 or CO2 inside the grains of the nanoparticles [9]. The broad absorption peak observed nearly at 3397.44 cm^{-1}related to OH functional groups [10]. The band between the region of 1000–1500 $cm^{-1}$are symmetric and asymmetric stretching vibrations which are contributed to O-C=O and C–O. The weak band near 1623.24$cm^{-1}$is assigned to H–O–H bending vibrations mode [11].

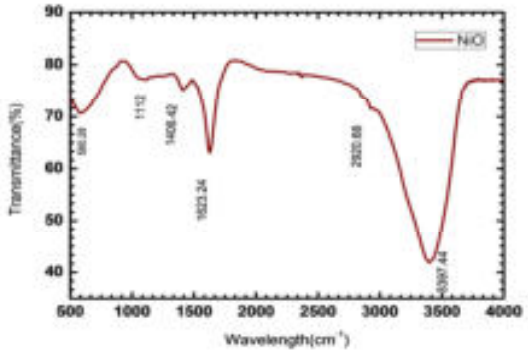

Figure-2. FTIR spectrum of NiO nanoparticles.

3.3. X-Ray diffraction (XRD) technique

The XRD pattern of prepared NiO nanoparticles depicted in **Figure-3**. The synthesized NiO nanoparticles exhibited crystalline structure with different diffraction angles. The diffraction peaks at 2θ= 31.42˚, 36.51˚, 52.59˚associated with (111,200, 220) crystal planes. The peaks at (211,221) were occurred due to impurity or presence of plant extract components. The crystalline size of the NiO nanoparticles were determined by Debye Scherer's equation, i.e., $D=k \times \lambda/\beta \times \cos\theta$. The size of the nanoparticles calculated from Debye Scherer's equation was 3.37nm (33.7A^{o}) with 2θ= 52.59˚ and the hkl plane was (220). The synthesized NiO nanoparticles were single crystalline having tetragonal cubic phase with a=b≠c. (JCPDS PDF No.: 73-1523) [12].

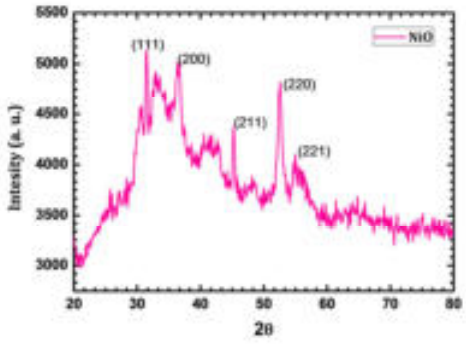

Figure-3. XRD pattern of NiO nanoparticles.

3.4. Antibacterial activity

The antibacterial activity of synthesized NiO nanoparticles was studied against microbial pathogens like Gram positive *Staphylococcus aureus* (*S. aureus*) and Gram negative *Escherichia coli* (*E.coli*). The simple agar well diffusion method was used

to study activity. The metal oxides like NiO enter into bacterial strain by diffusion mechanism and penetrate the cell wall of it. This penetration alters the structure of cellular membrane inner cellular components leads to cell death [13]. There are numerous mechanisms associated to antibacterial activity of NiO nanoparticles: - (i) generation of reactive oxygen species (ROS) which causes oxidative stress (ii) delocalization of membrane due to attachment of nanoparticles on bacterial cell membrane (iii) release of metal ions after binding to the bacterial membrane which was main cause of antibacterial activity [14]. Small particle size and minimum agglomeration effects on diffusion capacity and antibacterial efficiency of nanoparticles.The electrostatic interaction is present between negatively charged bacterial cell and positively charged nanoparticles.This interaction helps nanoparticles to enter into bacterial cell and may acts as bactericidal material.This entry of nanoparticle into cell generates reactive oxygen species leads to inhibition of bacterial growth. The increasing oxidative stress alters the structure of proteins, lipids, nucleic acids and stimulates the cell death [15].

In the current study, Gram positive *S. aureus* and Gram-negative *E. coli* were used to study antibacterial activity of NiO nanoparticles. After incubation of 24 hours the petri plates were observed for zone of inhibition. From the zone of inhibition, it was observed that NiO nanoparticles showed good antibacterial activity against Gram positive micro-organisms than Gram negative micro-organisms **Figure-4** and **Table-1** represented the information about antibacterial potential of NiO nanoparticles.

Table-1. Zone of inhibition by NiO nanoparticles.

Well no.	Sample	Bacterial strain	Zone of inhibition (mm)
1.	Control (50µl)	*S.aureus*	21±0.47
2.	NiO (50µl)		24±0.94
3.	NiO (100µl)		27±0.81
1.	Control (50µl)	*E.coli*	19±0.47
2.	NiO (50µl)		21±0.81
3.	NiO (100µl)		23±0.81

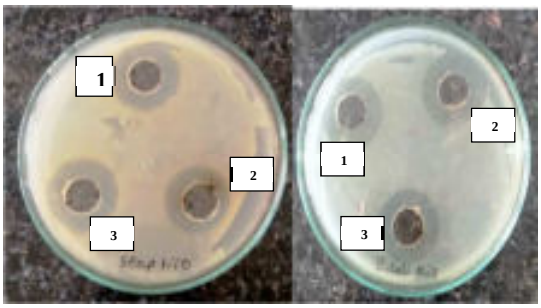

Figure-4. Zone of inhibition by NiO nanoparticles (a) *S.aureus*; (b)*E.coli.*

4. CONCLUSION

A novel green approach was carried out to synthesize NiO nanoparticles from tulsi leaves extract which has efficient reducing and capping properties. The structural properties were studied by using UV- visible spectroscopy, FTIR spectroscopy and X-ray diffraction technique. This work defines a specific procedure for the synthesis of NiO Nanoparticles based on cassava extracts. The antibacterial ability of NiO nanoparticles was studied against Gram positive and negative bacteria. It was found that, synthesized nanoparticles were potential antibacterial agent against Gram positive microbe than Gram negative. Thus, due to the eco-friendly and easy synthesis method, small size, single crystal nature and good antibacterial potential NiO nanoparticles can be used for various environmental and biomedical applications.

ACKNOWLEDGEMENT

We are very much thankful to the Department of Nanoscience and Technology, Y. C. I. S. Satara and Department of Biochemistry, Shivaji University, Kolhapur for providing all research facilities to carry out this work.

REFERENCES

1. Salvadori, M. R., Ando R. A., Nascimento, C. A. O., Correa1, B. (2015) Plos One, 10,1-15.
2. Mariam, A. A., Kashif, M., Arokiyaraj, S., Bououdina, M., Sankaracharyulu, M. G. V., Jayachandran, M., Hashim, U. (2014) Digest Journal of Nanomaterial and Biostructures, 9, 1007-1019.
3. Escobar, B., Lucio-Garcia, M. A., Barbosa, R., Morales-Acosta, D. (2018) Preprints, 9,1-6.

4. Tayade, U. S., Borse, A. U., Meshram, J. S. (2018) In International Journal of Scientific Research in Science, Engineering and Technology, 4, 43-49.
5. Pandian, C. J., Palanivel, R., Dhananasekaran, S. (2015) Chinese Journal of Chemical Engineering, 23, 1307-1315.
6. Ravindhranath, K., Ramamoorty, M. (2017) Rasayan Journal of Chemistry, 10, 716-722.
7. Kganyago, P., Mahlaule-Glory L.M., Mathipa M.M., Ntsendwana B., Mketo N., Mbita, Z., Hintsho-Mbita, N.C. (2018) Journal of Photochemistry and Photobiology B: Biology, 182, 18-26.
8. Wardani, M., Yulizar, Y., Abdullah, I., Apriandanu, D. (2019) Material Science and Engineering, 509, 012077.
9. Ezhilarasi, A., Vijaya, J. J., Kaviyarasu, K., Maaza, M., Ayeshamariam, A., Kennedy, L. J. (2016) Journal of Photochemistry and Photobiology B: Biology, 164, 352-360.
10. Khalil, A. T., Ovais, M., Ullah, I., Ali, M., Shinwari, Z. K., Hassan, D., Maaza, M. (2017) Artificial Cells, Nanomedicine and Biotechnology, 16, 1-16.
11. Panji, A., Simha, L. U., Nagabhushana, B.M. (2016) International Journal of Engineering and Management Research, 6, 287-291.
12. Nandapure, B. I., Kondawar, S. B., Nandapure, A. I. (2014) International Journal of Researches in Biosciences, Agriculture and Technology, 2437-2517.
13. Helan, V., Prince, J. J., Al-Dhabi, N. A., Arasu, M. V., Ayeshamariam, A., Madhumitha, G., Roopan, S. M., Jayachandran, M. (2016) Results in Physics, 6, 712-718.
14. Dhanuja, B. S., Devadathan, D., Baiju, V., Biju, R., Raveendran, R. (2017) International Journal of Advance Research in Science and Engineering, 162-167.
15. Umaralikhana, L., Mohamed, Jaffar, M. J. (2016) Journal of Advance Applied Scientific Research, 1, 24-35.

Ecofriendly and cost effective synthesis of silver nanoparticles by *Bacillus subtilis* NCIM 2010

Salma H. Nadaf [a], Sandip S. Kale[a], Pranoti N. Kirdat[a], Naiem H. Nadaf [b], Padma B. Dandge[a,*]

[a]Department of Biohemistry, Shivaji University, Kolhapur 416 004 (MS) India.
[b]Department of Microbiology, Shivaji University, Kolhapur 416 004 (MS) India.
*Corresponding author: pbd_biochem@unishivaji.ac.in

ABSTRACT

An economic and simple process of green silver nanoparticles synthesis was attempted by Bacillus subtilis NCIM 2010. The cell suspension of Bacillus subtilis NCIM 2010 prepared in sterile distilled water and utilised as mediator of silver nanoparticles fabrication at room temperature. The synthesis of particles occurs during incubation. The aqueous silver ions present in sterile distilled water getting reduced to their respective nanoparticles after 48 h of treatment at pH 7.0 and 30^{o}C. The structural characteristics of nanoparticles were revealed by various analytical procedures. Peak obtained at 430 nm in UV visible spectroscopic analysis confirms the presence of particles which is specified for its surface Plasmon resonance, Synthesized particles are in spherical form and having practical size ranging from 7 to 40 nm with average 17 nm and showed crystal nature. TEM analysis revealed surface anaionic charge on synthesized nano particles. These nanoparticles have characteristic broad spectrum antibacterial properties for different Gram negative and positive bacteria. However, there is a quite resistance showed by selective Gram-negative microorganisms.

KEYWORDS

Nanoparticles, Bacillus, Antibacterial, Silver nanoparticles.

…….

1. INTRODUCTION

Nanobiotechnology gained lots of attention in current decade because of its predictable influence in different fields like power, pharmaceutical, electrical devices and spacecrafts industry. From last decade this area of science increased its demand exceptionally around the globe [1]. Amongst all metalonanoparticles, AgNPs had various essential applications; because of its antibacterial and disinfecting properties and well known ever since Roman empire era. Though, advancement in synthesizing silver nanoparticles is increased because of its bactericidal properties [2] AgNPs shares one of the significant inputs at the era of bio-labelling, sensor technologies, microbicidal components and in filtration technologies. The silver nanoparticles also having potential to be safe utilized in water purification plants, in pesticide denaturation as well as in humans it acted as a potent agent for iradicating different disease causing virulent microbial pathogen. At present, the exploration of silver nanoparticle in antimicrobial treatment fact has gain attention because of increase in multiple drugs amongst microorganism [3].

Various physicochemical methodologies like electro-chemical, ultra sonication assisted, photo-chemical, reverse micelles, emission, etc. where been reported for fabrication of nanoparticles [4] but, these techniques has limitation of expensiveness and secondary pollution due to utilization of chemicals for synthesis and would exert toxicity to the natural flora-fauna and other biological entities of natural ecosystems and also to the environment [5] As biological or green synthesis of nanoparticles consumes different prokaryotes and eukaryotes organallies and cells and reported for having a good quality for have inorganic nanomaterial's fabrication by intracellularly or extra-cellularly with their biomineralization process of [6]. Microorganism assisted fabrication of silver nanoparticles is recognised as a renowned and hopeful method for exploitation of various kinds and properties bearing silver nanomaterials [7]

Manufacture of nano size metallic AgNPs with diverse structural properties and sizes by various route were been already documented the simple method for the AgNPs synthesis concerning a reduction of silver salts and these will be carried out by physical method involves reduction of an ionic salt in an suitable media with surfactant using various reducing agents, such as sodium borohydride [8] hydrazine hydrate, [9] sodium citrate, (Pillai et al., 2004)and ascorbic acid [10] there are different type of microorganism which were used for synthesis of AgNPs including bacteria, Fungi, actinomycets and fungi [11]. In this context we studied the synthesis of AgNPs by *Bacillus subtilis* NCIM 2010 its characterization and its antibacterial activities.

2. EXPERIMENTAL SECTION

2.1. Materials

Microorganism used- *Bacillus subtilis* NCIM 2010 was got from National Collection of Industrial Microorganisms (NCIM - Pune) India. Obtained pure strain repeatedly transferred grown and maintained on Nutrient agar at 4ºC during study *B. cereus* NCIM 2703; *S. aureus* NCIM 2654; *P. earuginosa* NCIM 5032; *P. vulgaris* NCIM 2813 and *S. typhi* NCIM 2501 were used for analysis of antibacterial activity of AgNPs, were grown on nutrient agar and maintained on same medium at 4 ºC until their use.

2.2. Synthesis of Silver nanoparticle

Growth of *Bacillus subtilis* NCIM 2010 was obtained by inoculating and grow organism in 250-mL conical having 100 mL nutrient broth at 30°C and 110 rpm on rotary shaking incubator for 24 h. completely incubated broth having cell density of 5×10^7 cells / mL was then centrifuged at 4000 X g for 10 min to obtain cell biomass. Collected biomass was then washed with sterile distilled water to make this biomass resudual component free and re-suspended gain same volume of (100 mL) in sterile distilled water with 1 mM $AgNO_3$, and allowed to incubate at 25°C after incubation cell free extracts were characterized by UV-visible spectrophotometry.

2.3. Analysis of AgNPs and its Characterizations

a. UV/visible spectroscopic investigation

The depiction of the silver nanoparticles was done by UV/Visible spectroscopy using a Hitachi U-2800 double beam spectrophotometer. The wavelength spectra of cell free extracts was taken starting from wavelength 300nm to 800nm and observed for the appearance of the peak in given wavelength. For determination of the maximum synthesis of AgNPs same experiment was done after interval of 6h from the inoculation point.

b. X-ray Diffraction studies

The purified crystalled powder of metal AgNPs was examined by X –ray diffraction using Philips analytical – PW3710, X ray diffractometer with a target CrKα (α = 2.28 Ao) the generator was operated at 40 Kv with a 25mA current. The scanning range (2θ) was 10o to 100 o.

c. TEM

The morphological characters of AgNPs were obtained monitoring silver nanoparticles for TEM. The analysis, of an aliquot of aqueous solution of silver nanoparticles was locate on copper grid which is carbon coated, sample is allowed to dry. Scanning of this grid done by with a Philips model (M200) Transmission electron microscope monitored at a current from 20 - 200 kV with 2- 4 Ao resolution.

d. Effect of pH and Temperature on AgNPs synthesis

To study various pH and Temperatures impact on AgNPs synthesis, AgNPs synthesis by microorganism was checked at diverse temperatures like 15, 20, 25, 30 35, 40 and 45oC and from pH 5.0, 6.0, 7.0, 8.0, 9.0 and 10 by monitoring an absorbance at 430 nm.

e. Antibacterial activity of AgNPs

Antimicrobial activity of AgNPs was tested against Gram negative bacterial strains, by agar well diffusion assay [12]. Inhibitory zones were noted after incubation.

f. Statistical analysis

Values obtained are mean of three or additional factors. Examination of the variants done by all data at $P < 0.05$ using Graph Pad software. (Graph Pad Instat version 3.00, Graph Pad software, San Diego, CA, USA).

3. RESULTS AND DISCUSSION

Aqueous solution of 1mM $AgNO_3$ supplemented with cell biomass which caused development of AgNPs within 12h due to reductive ability microorganisms on silver ions was visibly detected through colour change as colourless to greenish and greenish to yellowish brown. The extent of AgNPs synthesis was checked with UV/Visible spectroscopic technique by evaluating distinguished absorption peak was observed near about 430nm (**Figure-1**).

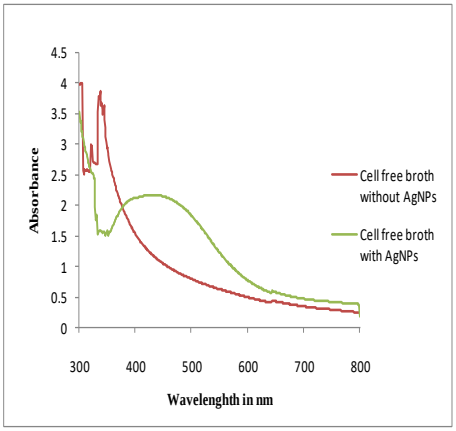

Figure-1. spectroscopic analysis of AgNPs synthesized by *Bacillus subtilis* NCIM 2010.

To determine maximum nanoparticles synthesis absorbance were recorded at the function of time with a definite time interval and the optimum absorbance was observed after 48 h and afterwards it remains constant (**Figure-2**).

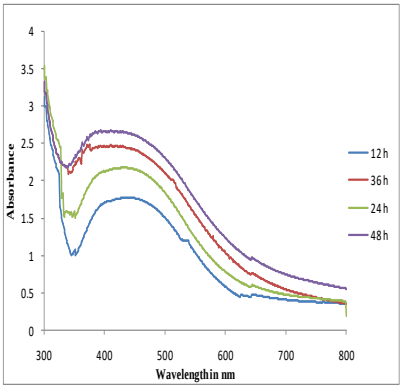

Fig.2

Figure-2. Synthesis of silver nanoparticles at different time interval of incubation.

Previous studies suggested that many bacteria having ability to produced AgNPs but duration of synthesis and its structural forms were different from each other such as *B. lechiniformis* has ability to synthesize the nanoparticles maximum in stationary phase [13]. *Bacillus Sp* produces Ag nanoparticles in their periplasmic space of the cell [8]. described production of AgNPs by yeast strain MKY3 in logarithmic phase [14]. elaborated the AgNPs synthesis with utilising spore crystals mixture of *Bacillus thurengenesis*. Other reports suggested that some bacteria synthesize nanoparticles extracellularly. *Pseudomonas stutzeri* intracellular synthesizing particle size approximately 200 nm [11,15], whereas AgNPs Synthesized by *Morganella sp*. were produced extracellularly and having size 20–30 nm [16], similarly silver and gold nanoparticles synthesis was carried out intracellularly by *Lactobacillus* strains [17] *Lectonemaboryanum* (Cyanobacteria) synthesizes Ag nanoparticles Intracellulary 1–10 nm [18].

The AgNPs exhibit an absorption spectral peak at 430nm at 12 h of reaction, in initial state after 6h medium starts to change the colour from transparent to green and after 9h it changes the colour from green to brown. The absorbance detected at 430nm is a typical SPR - band (surface plasmon resonance) of AgNPs and its observed so due to the excitation of longitudinal plasmon vibrations in silver nanoparticles [17, 19]. (**Figure-3**) shows forms of X-ray diffraction for the AgNPs. results display the incidence of diffraction peaks diffraction of face center cubic silver in the hole spectrum of 2θ value ranging from 10 to 80.

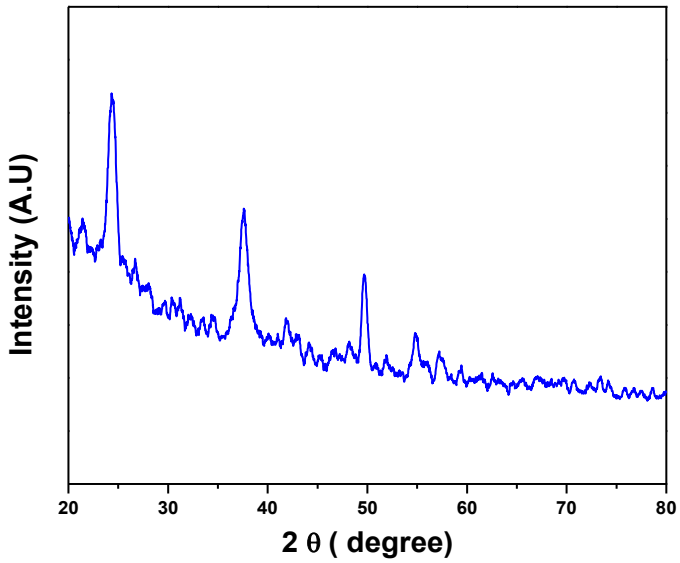

Figure 3. XRD evaluations of AgNPs synthesized by *Bacillus subtilis* NCIM 2010.

The average dimensions of crystalline AgNPs assessed by FWHM is (111) peak calculated by the Scherrer formula is 9.7 nm. On the scale of nanometer, maximum of face centered cubic (fcc) arranged metallic structures included silver were getting nucleated and grown within twinned and multiplied twinned AgNPs with their surfaces bounded by the minimum energic level (111) facets [20].

From TEM results (**Figure-4a**) it was exploited that AgNPs were mono-dispersed and round shaped. The particle size variation in size was seen in TEM micrograph (**Figure-4b)**. The synthesized AgNPs were found to have size in between of 7–40 nm and average 17 nm.

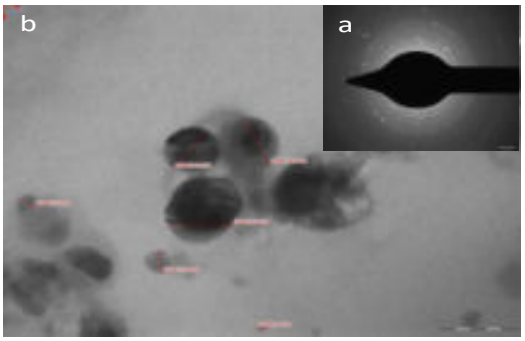

Figure-4. TEM analysis of AgNPs a) Inset: Selected area electron diffraction outline of AgNPs. b) TEM image of the AgNPs synthesize by *Bacillus subtilis* NCIM 2010 Scale bar corresponds to 50 nm.

From optimization studies it was revealed that *Bacillus subtilis* NCIM 2010 synthesize silver nanoparticles optimally at 7 pH and 30^{o}C. whereas best gold agumetation by microorganisms was normally occured in the 2–6 pH [11, 15] and variations in the pH has affected on the size of silver nanoparticles as shown in figure (**Figure-5**)

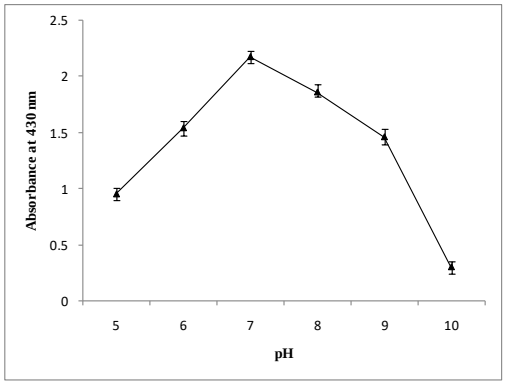

Figure-5. Synthesis of AgNPs at different pH.

and similar results are also observed in case of temperature optimization where the optimum temperature of AgNPs synthesis was 30^{o}C and for other temperature it was decreasing (**Figure-6**).

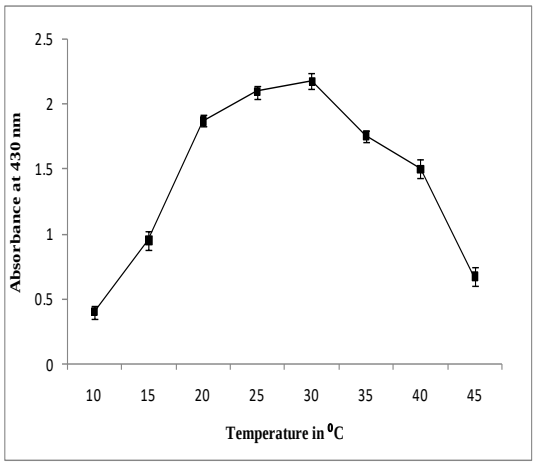

Figure-6. Synthesis of AgNPs at different Temperature.

It was revealed by previous studies that the silver nano particles possess antibacterial activity against of microorganisms selected from the ATCC strain collection and various another microorganism [21]. The antagonistic pattern of AgNPs on microbial cells showed to retard the DNA replication and translation processes so could impact on synthesis of some essential cellular and ribosomal proteins because of AgNPs action [22].

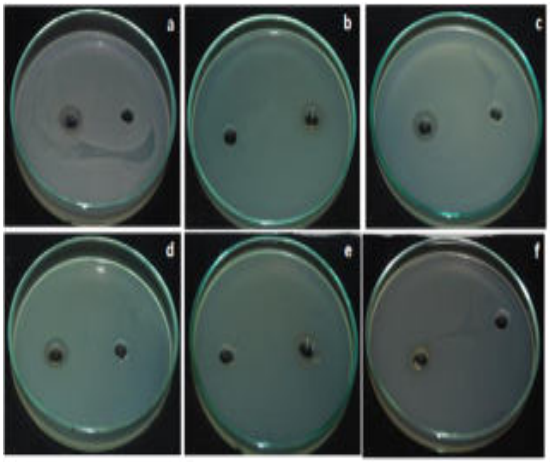

Figure-7. Antimicrobial activity of AgNPs on a) *Bacillus cereus* NCIM 2703 , b) *Staphylococcus aureus* NCIM 2654 , c) *Bacillus subtillis* NCIM 2635 d) *Pseudomonas earuginosa* NCIM 5032 e) *Proteus vulgaris* NCIM 2813 f) *Salmonella typphi NCIM 2654.*

(**Figure-7**) shows the results of antimicrobial activities it is seen that synthesized AgNPs shows the antimicrobial activities counter to some Gram negative and some positive bacteria. Within experimental microorganism zone of inhibition in diameter was observed against *Bacillus cereus* NCIM 2703, *Staphylococcus aureus* NCIM 2654, *Bacillus subtillis* NCIM 2635 and *Pseudomonas earuginosa* NCIM 5032 however *Proteus vulgaris* NCIM 2813 and *Salmonella typhi* NCIM 2654 does not show the zone of inhibition (**Figure-7; Table-1**). The increase in silver resistance in microorganism was observed due to extensive and abandoned use of Ag may result in more emerging bacterial resistant [23]. Though, these bacterial specificity in resistance within microorganism is depend on the possibility of transmission of Ag resistance gene and is lowest among other resistance [24, 25], that is the incidence of frequency of AgNPs is different amongst other organism [24]. Examination of the occurrence of silver resistance is very significant due to plasmid transfer and responsible for inter resistance amongst microorganism [3].

Table-1. Antimicrobial activity of AgNPs synthesized by *Bacillus subtilis* NCIM 2010.

Test microorganism	Zone of inhibition in diameter
B. cereus NCIM 2703	12 mm± 0.5
S. aureus NCIM 2654	13 mm± 0.2
B. subtillis NCIM 2635	16 mm± 0.3
P. earuginosa NCIM 5032	15 mm± 0.4

P. earuginosa NCIM 5032	-
S. typhi NCIM 2501	-

(-) = results not observed

Obtained results are the mean of three sets at (± SD) inhibitory impact of AgNPs shown to be significant from control as *P < 0.05.

4. CONCLUSION

In conclusion the cell suspension prepared in sterile distilled water of the *Bacillus subtilis* NCIM 2010 utilised as green synthesis of AgNPs with $AgNO_3$ at moderate temperature. It was anticipated that reductivity in silver ions is because of microbial production of different macromolecules especially proteins that may be contributed by the nitrate reductase enzyme. The structural characteristics of nanoparticles were revealed by various analytical procedures. The UV/Visible spectral analysis shown to have a spectral peak at about 430 nm, which typicaly observed for AgNPs. The AgNPs formed were round shaped with an average 17 nm particle size with crystal structure and anionic nature confirmed by TEM. The AgNPs seen to have large spectrum of antibacterial activities against various Gram-positive and negative bacteria but there is a resistance that observed in case of selective Gram-negative microorganisms which might be due to the extra chromosomal characteristics of that microorganism.

ACKNOWLEDGMENT

Authors Ms. Nadaf S.H, and other team members are thankful to Department of Biochemistry and Department of Microbiology, Shivaji University, Kolhapur, to extending their lab facilities for fulfillment of these work.

REFERENCES

1. Zhang, X., Yan, S., Tyagi, R. D., Surampalli, R. Y. (2011) Chemosphere, 82, 489-494.
2. Zhang, L., Jiang, Y., Ding, Y., Povey, M., York, D. (2007) Journal of Nanoparticle, 9, 479–489.
3. Woods, E. J., Cochrane, C. A., Percival, S. L. (2009) Veterinary microbiology, 138, 325-329.
4. Zhang, M., Cushing, B. L., O'Connor, C. L. (2008) Nanotechnology, 19, 085601.
5. Anastas, P. T., Warner, J. C. (1998) Green chemistry, 640, 30.
6. Feng, Q. L., Wu, J., Chen, G. Q., Cui, F. Z., Kim, T. N., Kim, J. O. (2000) Journal of biomedical materials research, 52, 662-668.
7. Jain, D., Kachhwaha, S., Jain, R., Srivastava, G., Kothari, S. L. (2010) Journal of Applied Polymer Science, 93, 1411.

8. Pugazhenthiran, N., Anandan, S., Kathiravan, G., Udaya Prakash, N. K., Crawford, S., Ashokkumar, M. (2009) Journal of Nanoparticle Research, 11, 1811-1815.
9. Pal, A., Shah, S., Devi, S. (2007) Colloids and Surfaces A: Physicochemical and Engineering Aspects, 302, 51-57.
10. Chaudhari, V. R., Haram, S. K., Kulshreshtha, S. K., Bellare, J. R., Hassan, P. A. (2007) Colloids and Surfaces A: Physicochemical and Engineering Aspects, 301, 475-480.
11. Klaus, T., Joerger, R., Olsson, E., Granqvist, C. G. (1999) Proceedings of the National Academy of Sciences, 96, 13611-13614.
12. Schillinger, U. (1989) Applied and environmental microbiology, 55, 1901-1906.
13. Kalimuthu, K., Babu, R. S., Venkataraman, D., Bilal, M., Gurunathan, S. (2008) Colloids and surfaces B: Biointerfaces, 65, 150-153.
14. Jain, D., Kachhwaha, S., Jain, R., Srivastava, G., Kothari, S. L. (2010) Journal of Applied Polymer Science, 93, 1411.
15. Joerger, R., Klaus, T., Granqvist, C. G. (2000) Advanced Materials, 12, 407-409.
16. Thakkar, K. N., Mhatre, S. S., Parikh, R. Y. (2010) Nanomedicine: Nanotechnology, Biology and Medicine, 6, 257-262.
17. Nair, B., Pradeep, T. (2002) Crystal growth and design, 2, 293-298.
18. Lengke, M. F., Fleet, M. E., Southam, G. (2007) Langmuir, 23, 2694-2699.
19. Mulvaney, P. (1996) Langmuir, 12, 788-800.
20. Allpress, J. G., Sanders, J. V. (1967) Surface Science, 7, 1-25.
21. Martinez-Gutierrez, F., Olive, P. L., Banuelos, A., Orrantia, E., Nino, N., Sanchez, E. M., Av-Gay, Y. (2010) Nanomedicine: Nanotechnology, Biology and Medicine, 6, 681-688.
22. Feng, Q. L., Wu, J., Chen, G. Q., Cui, F. Z., Kim, T. N., Kim, J. O. (2000) Journal of biomedical materials research, 52, 662-668.
23. Silver, S. (2003) FEMS microbiology reviews, 27, 341-353.
24. Summers, A. O., Jacoby, G. A., Swartz, M. N., McHugh, G, Sutton, L. In: Schlessinger, D. (1978) Journal of Microbiology, 67, 333-337.
25. Annear, D. I., Mee, B. J., Bailey, M. (1976) Journal of Clinical Pathology, 29, 441-443.

Phytochemical Analysis, in-vitro Antioxidant and Cytotoxicity capacity of *Ipomoea campanulata.*

Sandip S. Kale[a], Pranoti. N. Kirdat[a], Salma. H. Nadaf[a], Suresh S. Kale[b], Padma B. Dandge[a,*]

[a]Department of Biochemistry, Shivaji University, Kolhapur 416 004 (MS) India.
[b]Department of Botany, Sathaye College, Vile Parle, Mumbai 400 057 (MS) India.
[*]Corresponding author: pbd_biochem@unishivaji.ac.in

ABSTRACT

Ipomoea campanulata, a large shrubby climber plant collected from western ghat region covered under district Pune, Maharashtra to analyze antioxidant and cytotoxicity capacity of its extracts. The total phenolic content measured as gallic acid standard equivalent was found to be 0.440 ± 0.09 mg/ml and 0.380± 0.08mg/ml for methanol and ethyl acetate extract respectively. Flavonoid content was found to be 0.071 ± 0.002 mg/ml and 0.057± 0.002 mg/ml for methanol and ethyl acetate extract as Quercetin standard equivalent. The antioxidant potential of extracts was determined by employing DPPH Scavenging assay and Nitrous oxide radical scavenging assay. The highest % inhibition for DPPH scavenging (68.75 ± 1.08%) and Nitrous oxide radical scavenging (60.93 ± 6.93%) showed by methanolic extract and ethyl acetate extract of I. campanulata respectively. MTT assay showed that the methanolic extract is toxic to HepG2 and MCF 7 cells and their % inhibition are56.32% and 65.99% respectively. The study shows that the extracts of I. campanulata have strong antioxidant and cytotoxic capacity against HepG2 and MCF7 cells.

KEYWARDS

Ipomoea campanulata, Phytochemical, Antioxidant, Cytotoxicity.

……..……..

1. INTRODUCTION

In the plants, Convolvulaceae family contains nearly 1650 species from which approximately 500-600 species comprises by the genus *Ipomoea*. Hence, large numbers of species are from genus *Ipomoea* within the Convolvulaceae family [1]. The plants with heart-shaped leaves and funnel-shaped flowers under the twining or climbing woody or herbaceous plants dominate this genus. The most species of this genus *Ipomoea* are in the tropical region and some are in the temperate zones [2]. The *Ipomoea* genus has been studies for their phytochemicals from mid of 20th century. Some species of *Ipomoea* reported for their antimicrobial, analgesic, anticancer, spasmogenic, hypertensive and psychotomimetic activities. The common photochemical constituents that are ergoline alkaloids, nortropane alkaloids, glycolipids, coumarins, isocoumarin, phenolics compounds, norisoprenoids, diterpene, benzenoids, flavonoids, antocianosides, lignin and triterpenes has been identified as biological active constituents.

However, *Ipomoea campanulata* species is not well exploited for their phytochemical studies as well as biological activities [3].

The objective of this study is to phytochemically analyze *Ipomoea campanulata*, determine total antioxidant activity using 2-2 diphenyl-1-picrylhydrazyl (DPPH) & Nitric oxide radical scavenging, and characterize it through Liquid Chromatography- High Resolution Mass Spectroscopy (LC-HRMS). It is also includes cytotoxic properties of *I. campanulata* using HepG2 and MCF7 cell lines.

The general information regarding plant under study is as follows:

Classification: Kingdom – Plantae, Phylum – Tracheophyta, Class - Magnoliopsida Order – Solanales, Family – Convolvulaceae, Genus – *Ipomoea,* Species – *campanulata* L. viz *illustris* (C. B. Cl.) Prain

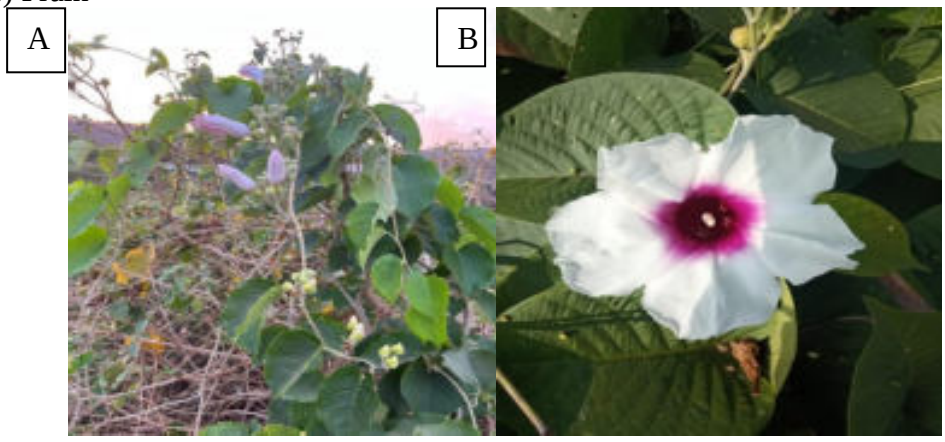

Figure-1. *Ipomoea campanulata* A) Plant B) Flower.

Ipomoea campanulata- Stout climbers with 8 x 9 cm leaves which are broadly ovate to orbicular, petiole to 8 cm long. Flowers are 1 or 2 together containing pedicels 3.5 cm long and stout. The sepals are 1 x 1 cm in size, orbicular in shape, outer 3 pubescent outside, growing in fruit; filaments hairy at base. Seeds are black and hairy on angles (**Figure-1**).

2. EXPERIMENTAL SECTION

2.1 Preparation of extract

The leaves of *Ipomoea campanulata* were collected from western ghat region covered under Pune, Maharashtra, India. Location lies in19°19'01.4"N 73°57'11.3"E. Dust particles were removed by washing leaves with tap water followed by distilled water. The leaves then shed dried for 15 days at room temperature and powdered using mechanical grinder. The crude extract was obtained by mixing 10 g of powder in 100 ml solvent keeping mixture overnight followed by filtration with Whatman No.1 filter paper. Crude extract concentrated by evaporating maximum solvent using rotavapor. Concentrated extract then taken on petriplates & evaporated completely. After obtaining yield, extract was re-dissolved in solvent for further use.

2.2 Phytochemical screening of extract:

The qualitative phytochemical tests were performed for Alkaloids, Anthraquinones, Proteins& amino acids, Saponins, Flavonoids, Phenols, Terpenoids, Sterols, Tannins and Glycosides to know their existence in plant extracts [4-6].

2.2.1 Test for alkaloids

One ml of plant extract was mixed with 1 ml Mayer's reagent. Yellow precipitation indicates the presence of alkaloids.

2.2.2 Test for anthraquinone

The 0.5 ml of plant extract added in 1 ml of 10 % ammonium solution, shaken vigorously for 1 min. Red color formation indicates the presence of anthraquinone.

2.2.3 Test for proteins and amino acids

Ninhydrin test – few drops of Ninhydrin reagent added in 1 ml plant extract, kept in boiling water bath for 30 sec to 1 min. Purple color formation indicates the presence of proteins and amino acids.

2.2.4 Test for Saponin

Foam test –
The 1 ml of plant extract shaken continuously for 15 min. Formation of layer of foam indicates the presence of saponin.

2.2.5 Test for flavonoids

H_2SO_4 test- few drops of conc. H_2SO_4 added in 1 ml of plant extract. Orange color formation indicates the presence of flavonoids.
Aluminium chloride test –In the adequate amount of plant extract equal amount of 1% aluminium chloride solution was added. The formation of light-yellow color indicates the presence of flavonoid.

2.2.6 Test for phenols

Ferric chloride test – 1 ml of plant extract mixed with 2 ml of 5% or 1 N aqueous ferric chloride. Formation of deep blue or black color indicates the presence of phenols.

2.2.7 Test for terpenoids

H2SO4 Test- 1 ml of plant extract mixed with 0.4 ml of chloroform, evaporate on boiling water bath, cool and added 0.6 ml conc. H_2SO_4, the solution was boiled for 30 sec. Formation of gray color indicates the presence of terpenoids.
Salkowski's test – In a solution of 1 ml plant extract and 2ml of chloroform, 3 ml of conc. H2SO4 added from the side of the test tube. The reddish-brown coloration at the interface indicates the presence of terpenoids.

2.2.8 Test for sterols

Salkowski's test – In a mixture of 1 ml plant extract and 2ml of chloroform, 1ml of conc. H2SO4 added from the side of the test tube. The chloroform layer appears red and the acid layer appears greenish yellow fluorescent this indicates the presence of sterols.

2.2.9 Test for tannins

Ferric chloride test –1 ml of plant extract diluted with distilled water in 1:1 proportion them 2 – 4 drops of 1 N ferric chloride solution was added. Black color formation indicates the presence of tannins.

2.2.10 Test for glycosides

Leibermann's test – In a mixture of 1 ml of acetic acid and 1 ml of chloroform, 1 ml of plant extract was added. Then conc. H_2SO_4 was added drop wise. The green color formation indicates the presence of glycosides.
Salkowski's test- 2 ml of conc. H_2SO_4 was added drop wise to the plant extract. The reddish-brown color formation indicates the presence of glycosides.

2.3 Total Phenolic Content

The total phenolic content in extracts was determined by Folin- Ciocalteu method [7]. Total phenolic content in extract presented as milligram Gallic Acid Equivalent (GAE).

2.4 Total Flavonoid Content

Total flavonoid content in plant extracts were estimated by method described by Khlif et al. [5]. Total Flavonoid content in extracts presented as milligram Quercetin equivalent.

2.5 Total Protein Content by lowry's method

The total protein content was evaluated by Lowry et al. [8] using BSA as a standard. The total protein content was expressed in mg/ml of extract.

2.6 Total Reducing Sugar Content by DNSA method

Determination of total reducing sugar content was done by DNSA method using glucose as a standard. The total reducing sugar content expressed in mg/ml of extract.

2.7 Antioxidant activity

2.7.1 DPPH radical scavenging activity

The DPPH free radical scavenging activity of extract was determined using methods described by Nguemfo et al. [9]. Briefly, 1ml of 1 mg/ml extract/Ascorbic acid added to 3 ml of a DPPH solution (0.004 % in methanol). Then mixtures were incubated in dark for 30 min. After incubation absorbance was recorded at 517 nm in a spectrophotometer using solvent as blank. The percentage inhibition of the DPPH radical calculated for extract and Ascorbic acid according to formula:

$$\% \text{ Inhibition} = [A_c - A_t]\, A_c \times 100$$

Where, 'A_c' is the absorbance of the DPPH control at t = 0 min and 'A_t' is the absorbance in presence of Extract/Ascorbic acid at a particular concentration at t = 30 min.

2.7.2 Nitric oxide radical scavenging activity

The Nitric oxide radical scavenging activity was evaluated by the method describe by Gangwar et. al., (2014) [10]. 1mg/ml of extract/Ascorbic acid added in 3 ml of 10 mM Sodium Nitroprusside (prepared in 0.5 M phosphate buffer (pH 7.4)). Mixtures were incubated for 150 min at 25^0C then1.0 mlGriess reagent [(0.33% sulfanilicacid in 20% glacial acetic acid)+ 1 ml of naphthylethylenediamine dichloride (0.1% w/v)] was added. Spectrophotometrically absorbance was measured at 546 nm. Thenitric oxide radical inhibition was calculatedusing followingformula:

% inhibition of NO radical= $(A_0 – A_t) /A_0$ X 100

Where, A_0 is the absorbance before reaction and A_t is the absorbance after reaction.

2.8 Detection of phytochemicals by LC-HRMS

LC-HRMS/MS phytochemical profiling was performed on an Agilent6540 UHDUHPLC system, diode array detector and electrospray ionization-quadrupole-time of flight mass spectrometer (ESI-QTOF-MS). An Agilent zorbax SB-C18 (150 X 0.5 mm, 5µ) column was used. The following gradient use: 0.1% formic acid in water (A), 0.1% formic acid in methanol (B). Injection volume was 10 µl, flow-rate was 0.5 ml/min. ESI-Q-TOF-MS analysis was done in positive ionization mode with mass range 100-1700 m/z [11-12].

2.9 Cytotoxicity capacity by MTT assay

Cytotoxicity of *I. campanulata* plant extracts was evaluated by using the method described by Abubakar et al. [13] and Ihmaid et al. [14] with modification. Cells with the concentration of 1 × 10^4cells/ml incubated in culture medium for 24 h at37°C with 5% CO2. In 100µl culture medium, cells were seeded as1 x10^4cells/well with the sample (100µl/ml) concentration 10, 40, 100 µg/ml. DMSO (0.2% in PBS) & cell line incubated in wells as control. To know the control cell survival and percentage of live cells after culture controls were maintained. The incubation of cell cultures was done for 24 h at 37°C and 5% CO2 in CO2 incubator (Thermo scientificBB150**).** Medium was completely removed after incubation, 20 µl of MTT reagent (5mg/min PBS) was added and cells were incubated for 4 hrs at 37^0C in CO2incubator. Formation of formazan crystals in the wells was observed under microscope. Viable cells reduced yellowish MTT into dark colored formazan. After incubation medium was removed completely and 200µlof DMSO added. Then kept for 10 min and again incubated at 37^0C (wrapped with aluminium foil). Absorbance of each sample was measured by a microplate reader **(**Benesphera E21) at a wavelength of 550 nm. The percent inhibition was calculated by using formula:

% Inhibition = [A(control) – A (extract/Standard)/ A(control)]* 100

3. RESULTS & DISCUSSION

The extraction of *Ipomoea campanulata* leaves were done by methanol (IC-Me) and ethyl acetate (IC-EA) solvents. For to know the presence of primary metabolites such as amino acids, carbohydrates, proteins, and secondary metabolites such as phenolics, flavonoids, saponins, tannins, terpenoids, glycosides, and anthraquinones etc. qualitative phytochemical tests were performed. **Table-1** shows the results of the qualitative phytochemical analysis.

Table-1. Qualitative phytochemical analysis of *I. campanulata* leaves extract. (+) Present, (-) Absent.

Constituents	Test	*I.campanulata*	
		IC-Me	IC-EA
Alkaloids	Test for alkaloids	+	+
Anthraquinones	Test for anthraquinone	-	-
Proteins and amino acids	Ninhydrin test	+	+
Saponins	Foam test	+	+
Flavonoids	i)H2SO4 test	+	+
	ii)Aluminum Chloride test	+	+
Phenols	Ferric chloride test	+	+
Terpenoids	i)H2SO4 test	+	+
	ii)Salkowski's test	+	+
Sterols	Test for sterol	+	+
Tannins	Ferric chloride test	+	+
Glycosides	i) Leibermann's test	+	+
	ii)Salkowski's test	+	+

The phytochemicals like phenolic, flavonoids, proteins and reducing sugars were analysed quantitatively. **Table-2** shows the results of the quantitative phytochemical analysis.
The antioxidant activityof *I. campanulata* leaves extracts were evaluated using DPPH & Nitric oxide free radical scavenging method.Ascorbic acid was used as a standard. **Table-3** represents the results of in-vitro Antioxidant activity.

Table-2. Analysis of total content of Phenolic, Flavonoid, Protein & Reducing sugar in *Ipomoea campanulata* leaves extract. Results were presented as Mean ± SD.

Sample (1 mg/ml)	*I. campanulata*	
	IC-Me	IC-EA
Total Phenolic content (Gallic acid equivalent inmg/ml)	0.440± 0.09	0.380± 0.08
Total Flavonoid content (Quercetin equivalent in mg/ml)	0.071± 0.002	0.057± 0.002
Total Protein content	0.013± 0.004	0.022± 0.006
Total Reducing sugar content	0.077± 0.009	0.092± 0.015

Table-3. Antioxidant activity of *Ipomoea campanulata*plant leaves extract. Results were presented as Mean ± SD.

	Antioxidant	
Sample 1mg/ml	DPPH Free Radical scavenging (% inhibition)	NO radical Scavanging assay (% inhibition)
Standard (Ascorbic acid)	74.46±1.62	78.12± 2.55
IC-Me	68.75±1.08	56.25±5.10
IC-EA	67.15±0.76	60.93±6.93

The phytochemicals detected from *I. campanulata* methanolic leaf extract by using the LC-HRMS/MS method are presented in **Table-4**. The greater number of compounds detected from phenolic, flavonoid, terpenes and terpenoids group.

Cytotoxicity analysis was done by MTT assay. The results of MTT assay are represented in **Table-5**.

The methanolic extract of *I. campanulata* showed a significant inhibition for HepG2 and MCF7 cells.

Table-4. List of bioactive components detected by LC-HRMS/MS in methanolic extract of *I. campanulata.*

Sr.No	Name of compound	RT	Mass	M/Z	Molecular Formula
1	Sebacic acid	0.49	202.1207	202.1444	C10 H18 O4
2	Pirbuterol	0.64	240.1477	241.1549	C12 H20 N2 O3
3	Trolamine	0.66	149.1058	132.1025	C6 H15 N O3
4	Brusatol	6.52	520.1952	503.192	C26 H32 O11
5	Myricitrin	6.57	464.0956	465.1032	C21 H20 O12
6	Quercetin	7.05	550.0964	551.1039	C24 H22 O15
7	(±)-Taxifolin	7.2	304.0586	287.0554	C15 H12 O7
8	Hymenoxon	8.11	282.1466	283.1539	C15 H22 O5
9	Zingerone	9.78	194.095	195.1024	C11 H14 O3
10	Sarcostin	1025	382.2358	365.2326	C21 H34 O6
11	Ricinoleic acid	11.36	298.2511	298.2744	C18 H34 O3
12	Populin	11.68	390.1318	373.1284	C20 H22 O8
13	Sphinganine	11.7	303.1473	302.3059	C18 H39 N O2
14	Heliotrine	11.75	313.1891	296.1857	C16 H27 N O5
15	Embelin	12.85	294.1834	277.1801	C17 H26 O4
16	Phytol	14.06	296.3082	314.3421	C20 H40 O
17	Graphinone	14.99	296.1624	279.1592	C16 H24 O5
18	Misoprostol	17.12	382.272	365.2695	C22 H38 O5
19	Lutein	20.53	568.4285	551.425	C40 H56 O2
20	Typhasterol	23.58	448.3561	431.3529	C28 H48 O4

Table-5. Results of cytotoxic activity on HepG2 and MCF7 cell lines with methanol extract of *I. campanulata*.

MTT assay					
Sample	Concentration (µg/ml)	Mean absorbance		HepG2 cell lines (% inhibition)	MCF7 cell lines (% inhibition)
		HepG2	MCF7		
	Control	0.973	1.538		
5FU (Std)	10	0.233	0.731	76.05	52.47
	40	0.214	0.673	78.00	56.24
	100	0.156	0.633	83.96	58.84
IC-Me	10	0.773	0.653	20.55	57.54
	40	0.657	0.589	32.47	61.70
	100	0.425	0.523	56.32	65.99

4. CONCLUSION

The present study revealed that, *I. campanulata* has a wide range of secondary metabolites with the higher phenolics and flavonoid content. The *I. campanulata* plant extracts showed the remarkable Antioxidant and cytotoxic activities. The confirmation of bioactive components in *I. campanulata* was done by LC-HRMS profile. Hence, *I. campanulata* can be act as a good source of the bioactive components. Exploitation and further studies of *I. campanulata* plant may help in identifying and purifying crude drug for medicinal use.

AKNOWLEDGEMENT

This work was supported by Research Strengthening Scheme, Shivaji University, Kolhapur (Maharashtra) (Ref.No:SU/C&U.D.Section/8/1324).

REFERENCES

1. Austin, D. F., Huáman, Z. (1996) Taxon, 45, 3-38.
2. Cao, S., Guzza, R. C., Wisse, J. H., Miller, J. S., Evans, R., Kingston, D. G. I. (2005) Journal of Natural Products, 68, 487-492.
3. Meira, M., Pereira da Silva, E., David, J. M., David, J. P. (2012) Revista brasileira de Farmacognosia, 22, 682-713.
4. Gul, R., Syed, U. J., Syed, F., Sherani S., Jahan N. (2017) The Scientific World Journal, 13, 5873648.
5. Khlif, I., Jellali, K.., Michel, T., Halabalaki, M., Learndros, A., Skaltounis, Allouche, N. (2018) Journal of Natural Medicine, 16, 354-357.
6. Santhi, K., Sengottuvel, R. (2016) International Journal of Current Microbiology and Applied Sciences, 5, 633-640.
7. Raghavendra, H. L., Kekuda, T. R. P., Akarsh, S., Ranjitha, M. C., Ashwini, H. S.

(2017) International Journal of Green Pharmacy, 11, 98-107.
8. Lowry, O. H., Rosebrough, N. J., Farr, A. L., Randall, R. J. (1951) Journal of Biological Chemistry, 193, 265.
9. Nguemfo, E. L., Dimo, T., Dongmo, A. B., Azebaze, A. G. B., Alaoui, K., Asongalem, A. E., Cherah, Y., Kamtchouing, P. (2009) Inflammopharmacology, 17, 37-41.
10. Gangwar, M., Gautam, M. K., Sharma, A. K., Tripathi, Y. B., Goel, R. K., Nath, G. (2014) Scientific World Journal, 11, 279451.
11. Vasincu, A., Luca, V. S., Charalambous, C., Neophytou, M. C., Skalicka-Wo_zniak, K., Miron, A. (2022) South African Journal of Botany, 144, 83-91.
12. Hatice, Kiziltas. (2022) Process Biochemistry, 166, 157-172.
13. Abubakar, A. N. F., Achmadi, S. S., Suparto, I. H. (2017) Asian Pacific Journal of Tropical Biomedicine, 7, 397-400.
14. Ihmaid, S. K., Alraqa, S. Y., Aouad, M. R., Aljuhani, A., Elbadawy, H. M., Salama, S. A., NadjetRezki, Ahmed, H. E. A. (2021) Bioorganic Chemistry, 111, 104835.

GUIDELINES FOR CONTRIBUTORS

1] **Journal of Shivaji University : Science & Technology** is the publication of Shivaji University, Kolhapur (Maharashtra, India), being published twice a year. It is an academic peer reviewed ISSN approved Journal.

2] The Journal welcomes research articles based on original research, review papers, research communication/notes by the faculty and research scholars working in various fields of Science and Technology. Articles/Papers can be submitted in English language only.

3] The length of manuscripts should not exceed 6000 words for review article, 5000 words for research article, 2000 words for research communication and 1000 words for research note.

4] The article/paper must accompany an **abstract not exceeding 200 words.**

5] During writing and submission of a manuscript, please follow the author guidelines arakble on the home page of Journal of Shivaji University: Science and Technology.

6] All the sources of literature referred to while writing the article/paper must be properly cited in the text. The serial numbers of End Notes, if any, must also be indicated within text at appropriate places.

7] The listing of references must follow the standard format.

8] Tables, charts, maps, figures etc. should be placed at appropriate places in the text of the article/paper and must be numbered serially with suitable headings. The tables should be referred to by their numbers within the text. Art-work for maps, figures and charts should be provided separately, if necessary.

9] Only articles evaluated and approved by the subject Experts/Referees/Departmental editorial board are considered for their publication in the Journal. The referees evaluate Article/ Paper drafts in term of structure and organization of paper/argument, originality of the research, appropriateness of abstract and introduction, literature review, methodology and data sources, data/evidence and conclusions, and quality of language.

10] The name of the author/co-author of the article being submitted should mentioned on the first page of the article/paper below title of that article. An asterisks (*) is used for defining corresponding author/s of a manuscript.

11] For any other information and for inquiries regarding submitted articles/papers preferably use e-mail communications. **(E-mail : editor.jscitech@unishivaji.ac.in)**

12] Manuscript should be sent to email of the Editor (**editor.jscitech@unishivaji.ac.in**) {or associate editor of the concerned subject}, Journal of Shivaji University: Science and Technology, Kolhapur with e-copy only (single M.S. word as well as PDF file).

Only research articles/review papers/research communication/notes prepared strictly in accordance with the above guidelines will be sent to referees for their evaluation and opinion about their acceptability or otherwise. We do not send back rejected articles.

शिवाजी विद्यापीठ कोल्हापूर
ज्ञानमेवामृतम्